[American Journal of Science, Vol. 313, May, 2013, P. 395–451, DOI 10.2475/05.2013.01]

American Journal of Science

MODELING SPECIFIC pH DEPENDENT SORPTION OF DIVALENT METALS ON MONTMORILLONITE SURFACES. A REVIEW OF PITFALLS, RECENT ACHIEVEMENTS AND CURRENT CHALLENGES

CHRISTOPHE TOURNASSAT*,†, SYLVAIN GRANGEON*, PHILIPPE LEROY*, and ERIC GIFFAUT**

ABSTRACT. **Within the context of the clay barrier concept for underground nuclear waste disposal, montmorillonite and bentonite have been widely used as reference materials for sorption. In some cases, accompanying modeling work aims at understanding and predicting sorption in complex natural systems where clays are assumed to be representative of the most reactive phases. This bottom-up approach relies heavily on good confidence in the mechanistic understanding of sorption phenomena. The present study aims at reviewing experimental and modeling work on montmorillonite with a focus on divalent metals experiencing pH dependent specific sorption. Current knowledge points out distinct sorption mechanisms on three types of sites: cation exchange on basal planes and surface complexation on edge surfaces with two types of sites: high energy (or strong) sites (HES) with high affinity for metals but low site density and low energy (or weak) sites (LES) with lower affinity for metals but high site density. Based on this current knowledge, criteria are given to select data relevant for surface complexation model calibration (especially ionic strength, pH, clay preparation and characterization, metal to clay ratio and solubility limits), with an emphasis on data uncertainties and reproducibility. Problematic experimental features are highlighted, especially those related to the reversibility of sorption and to the effect of the solid to liquid ratio (R_{SL}) on sorption distribution coefficients. Guidelines for data acquisition and selection are proposed.**

Surface complexation models available in the literature are then tested in terms of efficiency (data fit) and mechanistic likelihood. None of the currently available models is able to satisfy both aspects. Models directly adapted from oxide surface complexation models fail in both aspects. The most efficient model (in terms of simplicity and accuracy) is a non-electrostatic model. It is the only one that reproduces pH dependent specific sorption data at a low metal clay ratio (<0.001 mol/kg$_{clay}$; HES) in all selected experimental conditions, as well as data obtained at medium metal to clay ratio ($\sim$0.01-0.05 mol/kg$_{clay}$; low energy sites). To account for physical mechanisms, an electrostatic surface complexation model has been developed. It takes into account the spill-over effect of negatively charged basal surfaces over edge surfaces, a typical feature of montmorillonite, and is able to reproduce sorption data for LES but not for HES. The reasons for this failure are explained through the mathematical derivations of model equations. This approach shows that it is impossible to reconcile HES properties with an oxide-like surface complexation electrostatic model. Amongst other alternatives, a successful electrostatic surface substitution model, which is compatible with current knowledge on HES structural properties, is proposed.

Key words: Sorption, clay, montmorillonite, metals, experimental data, efficient models, mechanistic models, surface complexation

* BRGM, 3 Avenue Claude Guillemin, 45060 Orléans Cedex 2, France
** Andra, 1 Rue Jean-Monnet, 92298 Châtenay-Malabry, France
† Corresponding author: c.tournassat@brgm.fr; BRGM, D3E/SVP, 3 Av. Claude Guillemin, BP 6009, 45060 Orléans Cedex 2, France; Tel: +33 2 38 64 47 44; Fax: +33 2 38 64 30 62

INTRODUCTION

Context

With the rise of the clay barrier concept for underground nuclear waste disposal, many studies have, since the 1990s, conducted sorption (that is absorption and adsorption) experiments of radionuclides (or their stable isotopes) on clay materials. Montmorillonite and bentonite have been widely used as reference materials for these studies, since they are assumed to be representative of the most reactive natural phases in the potential underground disposal sites (ANDRA, 2005). Over time, the studied systems have grown in complexity in order to take into account the complex mineral assemblages encountered in clay-rich rocks (Wolthers and others, 2006) as well as the competition effect between cations (Bradbury and Baeyens, 2005a) or the effects of natural humic and fulvic acids (Glaus and others, 2005; Bellenger and Staunton, 2008; Xu and others, 2008b). Last but not least, the effect of compaction on sorption properties is currently being explored in order to assess whether retention experiments performed on suspended powdered materials are representative of *in situ* conditions (Montavon and others, 2006; Van Loon and Glaus, 2008; Miller and Wang, 2012). The interpretation of these sorption experiments, conducted with complex systems, often relies on the use of numerical "mechanistic" modeling (Bradbury and Baeyens, 1997b; Kraepiel and others, 1999; Kulik, 2002a, 2002b; Ikhsan and others, 2005; Grambow and others, 2006; Montavon and others, 2006; Marcussen and others, 2009; Tertre and others, 2009). However, a clear mechanistic understanding of the sorption phenomena occurring in complex systems should rely on a sound comprehension of the phenomena involved in simple systems, for example with "pure" montmorillonite.

A survey of the literature available on pure montmorillonite systems demonstrates that all of the published models reproduce quite satisfactorily accompanying data. However, studies that test one of these models on a large dataset originating from different literature sources are very rare. Most often, all of the modeled data originates from the laboratory of the model's authors, with rare but notable exceptions (Bradbury and Baeyens, 2005b; Grambow and others, 2006). Discrepancies between existing models lie in their representation of clay surface reactivity and not all of their features are necessarily physically correct, although the models can successfully reproduce the data.

This article reviews main clay sorption models and experimental data. Among the various sorption/uptake processes, this review focuses on pH dependent specific sorption mechanisms. Nonetheless, other uptake processes will also be presented in order to discuss data available in the literature and identify those that could be used for model calibration.

Article Outline

The first section aims to provide an overview of (i) sorption processes taking place at montmorillonite surfaces and (ii) modeling approaches that are available to quantify sorption properties. In so doing, we highlight fundamental differences between montmorillonite and (oxyhydr-)oxides, for which surface complexation modeling approaches were initially developed following the reference works of Stumm, Schindler and co-workers (Stumm and others, 1970; Schindler and Gamsjager, 1972; Schindler and Stumm, 1987), Sposito (1984), Dzombak and Morel (1990), Sverjensky (1993), or Hiemstra and Van Riemsdijk (1989, 1996). It is demonstrated that these oxide models must not be applied to montmorillonite. In the second section, we provide a detailed analysis of the input parameters needed for a mechanistic surface complexation model, again emphasizing the peculiarity of the montmorillonite material as compared to oxides. In a third section, sorption data is reviewed with special

attention paid to the experimental conditions that enable a maximum of information on pH dependent specific sorption mechanisms to be obtained. We propose a selection of reliable sorption data that are relevant for our purposes and we highlight some pitfalls frequently encountered in the literature. In addition, some problematic experimental features are addressed that could not be solved on the basis of available reported results (for example, sorption reversibility). We also provide some guidelines for using relevant parameters and identifying missing information that cannot be constrained by currently available experimental approaches. In the last section, two modeling approaches are presented. The first modeling approach relies on simplicity and efficiency, following a parsimony rule with regard to fitting parameters, while the second relies as closely as possible on a physically correct description of the system. The limitations and strengths of both approaches are discussed. In the conclusions section, important messages (from our point of view) related to experimental procedures, input parameter constraints and model features are summarized in an attempt to provide a guideline for future studies.

SORPTION PROCESSES AND MODELING APPROACHES FOR MONTMORILLONITE SURFACES

Sorption Basics

Sorption results rely on knowledge of an initial added concentration (C_{init}) for the metal (Me) tracer and its concentration measurement at the end of the equilibration period (C_{eq}). The extent of sorption is usually evaluated in terms of (i) sorption percentage (%sorption, dimensionless), (ii) surface coverage (C_{sorb}, in mol kg^{-1}) and (iii) distribution coefficient (Rd or K_d, in L kg^{-1}) according to, respectively:

$$\%\,sorption = 100 \times \frac{C_{init} - C_{eq}}{C_{init}} \tag{1}$$

$$C_{sorb} = \frac{C_{init} - C_{eq}}{R_{SL}} \tag{2}$$

$$Rd = \frac{C_{init} - C_{eq}}{C_{eq} R_{SL}} \tag{3}$$

where R_{SL} is the solid to liquid ratio of the experiment (kg L^{-1}). These three sorption quantification modes are usually plotted (i) as a function of pH with a constant total Me concentration and a constant ionic strength or (ii) as a function of equilibrium Me concentration with a constant pH and ionic strength. In the following, non-dimensional ionic strength will be used (Solomon, 2001):

$$I = 0.5 \sum_i z_i^2 \frac{m_i}{m_i^0} \tag{4}$$

where z_i is the charge number of ion i, m_i is the molality of i and m_i^0 is the standard state (1 mol/kg_{H_2O}).

Overview of Sorption Processes on Montmorillonite

Montmorillonite is a 2:1 clay type mineral and its structure is composed of a sheet of aluminium cations in octahedral conformation ("O" layer), sandwiched between two sheets of Si cations in tetrahedral conformation ("T" layer). The layers formed by this assemblage are separated from the adjacent ones by an interlayer space containing water molecules. Substitutions of octahedral Al^{3+} or tetrahedral Si^{4+} by cations of lower

valences provide this mineral with a layer charge, compensated by interlayer cations in the interlayer space (Sposito, 1984, fig. 1). In the case of montmorillonite, the expandable interlayer space can accommodate a varying amount of water molecules (Ferrage and others, 2005a).

Oxygen atoms at TOT layer edges have fewer metal neighbors than in the bulk (White and Zelazny, 1988). This results in an edge charge that is dependent on physical and chemical conditions (mostly pH and ionic strength). Oxygen atoms at the edge can gain or lose protons to form surface hydroxyl groups and thus exhibit pH dependent surface charge and electrostatic potential.

The understanding of cation retention processes at clay surfaces has been a matter of considerable research effort over several decades. Following earlier work on clay cation exchange properties (from Thomson, 1850), identification of clay material properties with respect to trace metal retention was achieved through the measurement of sorbed amounts of zinc (Zn) that were not exchangeable by neutral salts (Jones and others, 1936; Hibbard, 1940; Brown, 1950) whereas they were extracted with salt solutions of increasing acidity (Brown, 1950). Similar findings were also made for copper (Cu–De Mumbrum and Jackson, 1956) and cobalt (Co–Spencer and Gieseking, 1954). Tiller and Hodgson (1960) further demonstrated, by means of sorption experiments, that specifically bound Co (as opposed to non-specifically bound metal, which can be exchanged by other cations such as ammonium) can be split into two forms. A dominant part of Co is extracted by moderate acid extraction (dilute acetic acid) and a very minor part is not. This last reservoir was assigned to trace metal cations having entered the TOT layer. Following these earliest works, non-specific and specific sorption processes, corresponding to sorption on, respectively, basal and edge surfaces of clay TOT layers, have been identified (Peigneur and others, 1975). Spectroscopic methods have shown that sorption on basal surfaces is mainly governed by cation exchange processes with outer-sphere complexes and thus strongly depends on ionic strength and on the ionic background composition (for example Na *versus* Ca). Sorption of divalent metallic cations also takes place through the formation of inner-sphere complexes. This mechanism is cation specific and depends mainly on pH. (Polarized) extended X-ray absorption fine structure (P-EXAFS) studies have demonstrated that these inner-sphere mononuclear surface complexes are present on the edges of tri- and di-octahedral smectites (Papelis and Hayes, 1996; Schlegel and others, 1999b; Schlegel and others, 2001a; Dähn and others, 2003). Increasing pH, Si concentration and/or ageing time (with subsequent dissolution of the clay and Si release in solution) initiates surface precipitate formation, including neo-formed phyllosilicates (Scheidegger and others, 1997; Schlegel and others, 2001b; Dähn and others, 2002; Lee and others, 2004; Schlegel and Manceau, 2006). Finally, Dähn and others (2011) and Churakov and Dähn (2012) demonstrated with P-EXAFS coupled to *ab initio* modeling the existence of two distinct groups of edge surface binding sites. This finding gave rise to the concept of high energy (or strong) sites (HES hereafter) and low energy (or weak) sites (LES hereafter) for surface complexation on clay edge surfaces that was introduced by Bradbury and Baeyens (1997b) for montmorillonite on the basis of sorption isotherm modeling.

Table 1 summarizes important spectroscopic results obtained as a function of experimental conditions and figure 2 shows how the different sorption processes on montmorillonite surfaces take place as a function of pH at constant Me concentration. At low pH, sorption is dominated by cation exchange on basal/interlayer surfaces. With increasing pH, sorption takes place first on HES whose affinity for divalent metals is high. If the metal to clay ratio is sufficiently high (that is compatible with a saturation of HES), a further increase in pH leads to sorption on LES whose affinity for divalent metal cations is lower than HES but whose site density is higher. At even higher pH

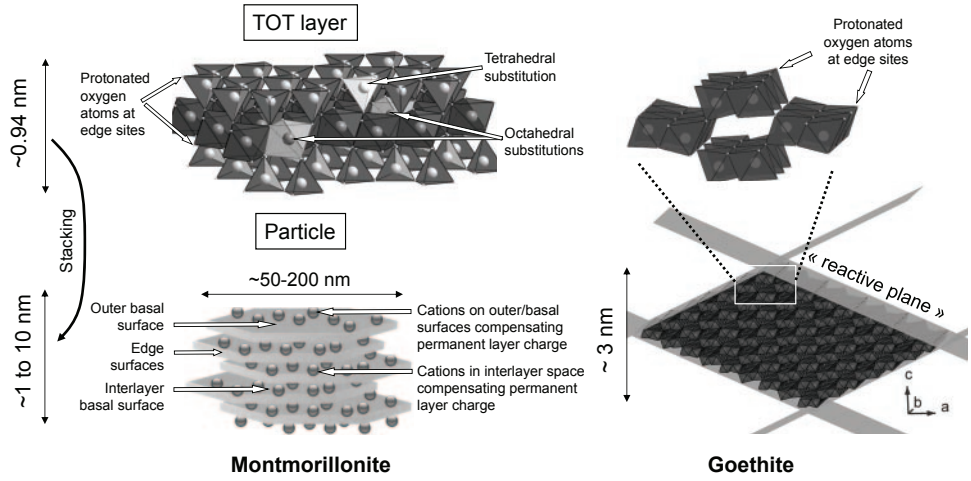

Fig. 1. Comparison of montmorillonite TOT layer structure and goethite structure with origin and localization of reactive sites. Modified from Tournassat and others (2011).

and/or metal concentration, co-precipitation phenomena can occur. At constant pH value and high ionic strength, HES contribution to sorption is predominant at low Me equilibrium concentration (fig. 3, top). When Me concentration increases, HES become saturated and LES, with lower Rd, become predominant in the overall sorption. Finally, at higher concentration, HES and LES are saturated and cation exchange becomes the dominant process, if no precipitation occurs. At low ionic strength, cation exchange can be the dominant process in all conditions (fig. 3, bottom). This schematic view of sorption processes highlights the need to choose carefully the experimental conditions and thus the datasets to test the various models available in the literature. For instance, HES properties can be probed only with (i) high ionic strength conditions (otherwise the contribution of HES to sorption can be masked by the contribution of cation exchange sites), (ii) a low ratio of total metal concentration over clay content (otherwise, the LES contribution can mask the HES contribution) and (iii) an adequate pH.

Clay surfaces exhibit some features similar to oxides but also notable differences. On the one hand, the concept of strong and weak sites is also used in models for oxide surfaces in order to describe differences in surface reactivity at low and high surface coverage of sorbing species. On the other hand, the permanent surface charge in the montmorillonite TOT layer has no equivalent in "conventional" oxide materials and the duality of sorption mechanisms on two types of surfaces having very different shapes and positions is a feature that is typical of clay minerals.

An Overview of Surface Complexation Modeling on Montmorillonite

Cation exchange reaction modeling must be taken into account as part of the overall sorption process (figs. 2 and 3). However, this review focuses on pH dependent specific sorption processes. Thus, the cation exchange reaction modeling approach is presented in Appendix 1.

pH dependent specific sorption on montmorillonite has been modeled by numerous authors using surface complexation models derived from oxides. In surface complexation models, sorbed species react chemically with surface hydroxyl groups

Table 1

Summary of spectroscopic results for discriminating divalent metal sorption processes at the montmorillonite surface

Study	Sorbed species	Loading (mmol kg^{-1})	Ionic background	pH	Spectroscopic methods and results
Papelis and Hayes, 1996	Co	200	0.001, 0.1 and 1 M $NaNO_3$	3 to 10	EXAFS: (1) outer-sphere, mononuclear surface complexes at low pH and low Na concentrations (2) inner-sphere, polynuclear complexes at higher pH and higher Na concentrations
Morton and others, 2001	Cu	40	0.1 M $NaNO_3$	6.2	EXAFS: Cu-Cu pairs
Dähn and others, 2002	Ni	25 (24 h)	0.2 M $Ca(NO_3)_2$	8	P-EXAFS: Ni-Ni pairs
	Ni	45 to 110 (14 to 206 d)	0.2 M $Ca(NO_3)_2$	8	P-EXAFS: Neoformation of Ni-phyllosilicate
Dähn and others, 2003	Ni	4 to 7	0.3 M $NaClO_4$	7.2	P-EXAFS: Ni sorbed on clay edges. Slight increase in retention with time without incorporation in the matrix. Sorbed species are more and more ordered at the surface with time
Schlegel and Manceau, 2006	Zn	50	0.5 M NaCl	7.3	P-EXAFS: Sorption in continuity with the octahedral layer. No Zn-Zn pairs
	Zn	130	0.5 M NaCl	7.3	P-EXAFS: Precipitation of Zn-phyllosilicates upon basic silica solution addition.
Dähn and others, 2011	Zn	~2.5	0.2 M $NaClO_4$	7.1	P-EXAFS: Sorption on high affinity edge sites (HES). Sites in continuity with the octahedral layer.
	Zn	32	0.2 M $NaClO_4$	7.1	P-EXAFS: Sorption on low affinity edge sites (LES). No Zn-Zn pairs. Sites not strictly in continuity with the octahedral layer.
Churakov and Dähn, 2012	Zn	~2.5 and 32	0.2 M $NaClO_4$	7.1	P-EXAFS data from Dähn and others (2011) in combination with atomistic simulations: (1) for HES Zn is incorporated into the outermost trans-octahedra on (010) and (110) edges (2) for LES, Zn forms mono- and bi-dentate inner-sphere surface complexes attached to the octahedral layer of (010) and (110) edge sites

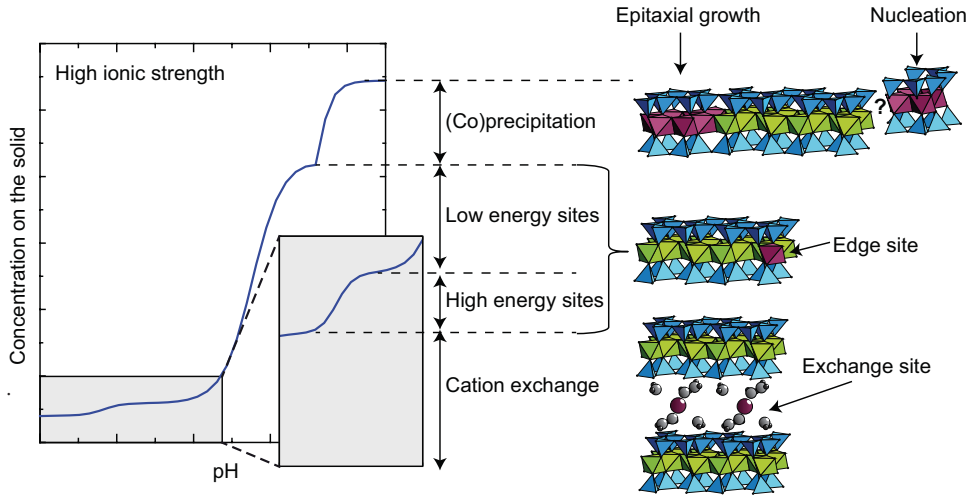

Fig. 2. Relative importance of identified sorption processes as a function of pH (schematic view). Decreasing ionic strength results in a higher contribution of cation exchange processes in the overall retention.

after coming through the interfacial electric field at the surface. The sorption of a divalent metal at a surface hydroxyl group is described by analogy to the formation of a soluble complex (reaction 1 is one of many possible reactions to form a surface complex):

$$>\mathrm{SOH} + \mathrm{Me}^{2+} \rightleftharpoons >\mathrm{SOMe}^{+} + \mathrm{H}^{+} \qquad K_{Me}^{int} \qquad \text{Reaction 1}$$

with:

$$K_{Me}^{int} = \frac{(\rangle\mathrm{SOMe}^{+})(\mathrm{H}^{+})}{(\rangle\mathrm{SOH})(\mathrm{Me}^{2+})} \tag{5}$$

where terms in parentheses refer to activities. The definition of surface species activity is problematic. In early versions of surface complexation models, surface species activities were related to their concentrations on the surface and to the surface potential (Ψ_i) experienced by the species i, by taking into account the electrostatic work necessary for the transport of ions through the electrostatic potential gradient from the bulk solution to the surface. The electrostatic potential is derived from the mean field approximation.

$$(\rangle\mathrm{SOMe}^{+}) = [\rangle\mathrm{SOMe}^{+}]\,exp\left(\frac{2F\Psi_{Me}}{RT}\right) \tag{6}$$

$$(\rangle\mathrm{SOH}) = [\rangle\mathrm{SOH}]\,exp\left(\frac{F\Psi_{H}}{RT}\right) \tag{7}$$

where terms in square brackets refer to concentrations, F is the Faraday constant (96 485 C mol^{-1}), R the gas constant (8.314 J mol^{-1} K^{-1}) and T the temperature (in K). This molarity convention leads however to thermodynamically unsatisfactory results for site/metal stoichiometries different from one. As an example, let us consider the following reaction:

$$2 >\mathrm{SOH} + \mathrm{Me}^{2+} \rightleftharpoons (>\mathrm{SO})_2\mathrm{Me} + 2\mathrm{H}^{+} \qquad K_{Me,heter}^{int} \qquad \text{Reaction 2}$$

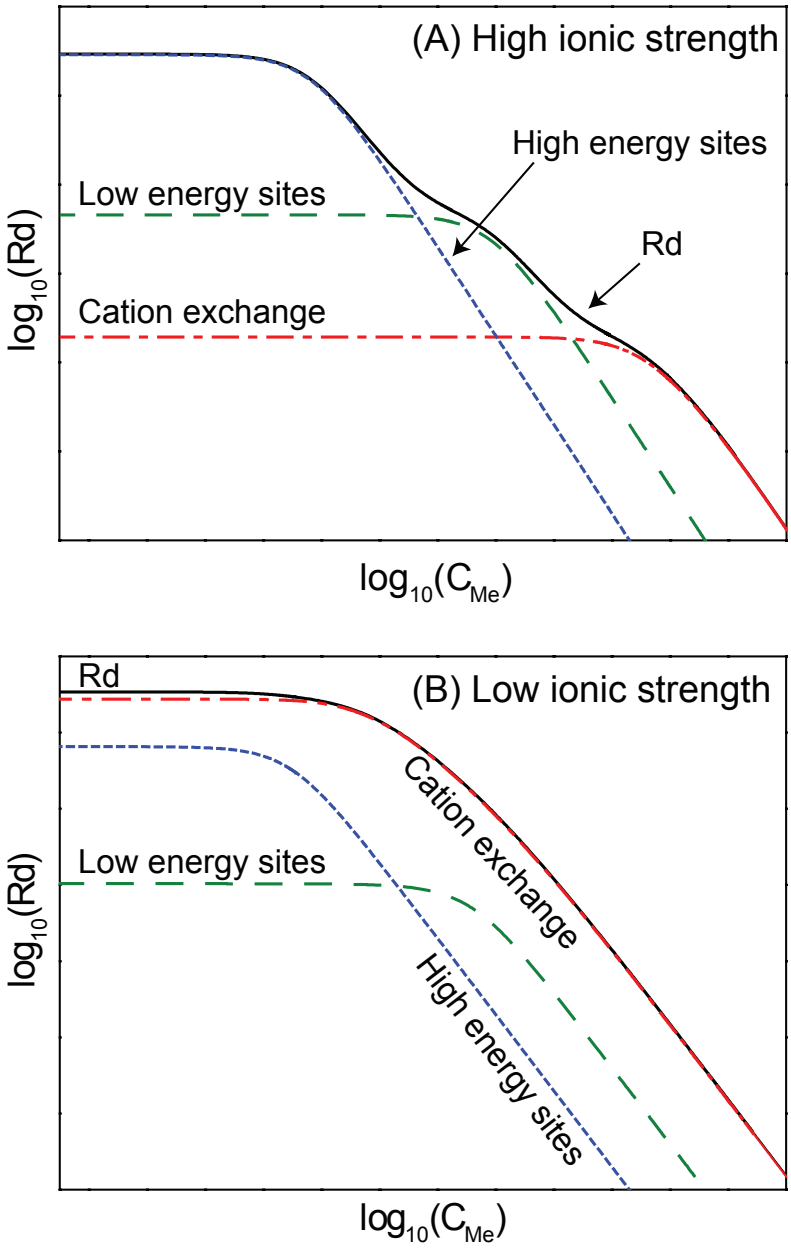

Fig. 3. Evolution of the distribution coefficient as a function of equilibrium Me concentration at low and high ionic strength (schematic view).

The use of the molarity convention leads to:

$$K^{int}_{Me,heter} = \frac{[(\rangle SO)_2 Me](H^+)^2}{[>SOH]^2(Me^{2+})}. \quad (8)$$

Equation (8) implies that, keeping constant solution conditions, that is with constant $\frac{(H^+)^2}{(Me^{2+})}$ ratio, if the solid/liquid ratio changes, then the composition of the surface will

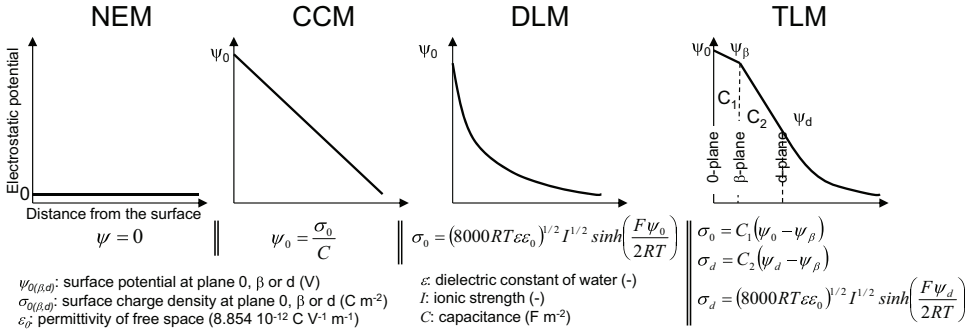

Fig. 4. Schematic representation of the electrostatic double layer at the clay surface/water interface and corresponding models relating surface charge densities to electrostatic potentials. NEM, CCM, DLM and TLM refer to non-electrostatic, constant capacitance, double layer and triple layer models respectively.

change. It is as if, for the analogous partitioning in gas-water systems, Henry's constant is dependent on the volume of the gas phase (Di Toro and others, 1986). This is not thermodynamically correct. This problem has been acknowledged for years (for instance, it is discussed in the PHREEQC manual–Parkhurst and Appelo, 1999) and has been addressed very thoroughly in Sverjensky (2003) and Kulik (2009). Still, there is no unifying theory to calculate the activity coefficients of surface species. In the following, we will rely on the mole ratio form of activity in surface complexation theory, where activity is related to the site molar ratio that is occupied by the metal, a non electrostatic surface activity coefficient (γ_{surf}) and an electrostatic surface coefficient term:

$$(\rangle \mathrm{SOMe}^{+}) = \gamma_{surf}^{\rangle \mathrm{SOMe}^{+}} \frac{[\rangle \mathrm{SOMe}^{+}]}{\sum_i [\rangle \mathrm{SOA}_i^{z_i - 1}]} exp\left(\frac{2F\Psi_{Me}}{RT}\right) \tag{9}$$

$$(\rangle \mathrm{SOH}) = \gamma_{surf}^{\rangle \mathrm{SOH}} \frac{[\rangle \mathrm{SOH}]}{\sum_i [\rangle \mathrm{SOA}_i^{z_i - 1}]} exp\left(\frac{F\Psi_{H}}{RT}\right) \tag{10}$$

where A_i refers to chemical species with charge z_i. The non-electrostatic surface activity coefficient is set at an arbitrary value of 1 in the absence of theoretical methods to calculate it (and of an experimental method to measure it). The surface electrostatic potential term depends (i) on the location of the sorbed species (inner-sphere, outer-sphere, diffuse layer) and/or (ii) on the electrostatic interface model used to calculate it. For example, early work on montmorillonite by Stadler and Schindler (1993) and Charlet and others (1993), on Cu and Al sorption respectively, were performed using a constant capacitance model (CCM). Zachara and Smith (1994) used a triple layer model (TLM) to fit Cd sorption. Marcussen and others (2009) used a double layer model (DLM) and Bradbury and Baeyens (1997b) have applied a simplified non-electrostatic model (NEM). The electrostatic double layer structures of these models are depicted in figure 4 together with equations relating the surface charge density to the electrostatic potential. The parameters that are necessary for model computations are given in table 2. All of these modeling approaches were adapted from surface complexation models that were developed successfully for oxides and hydroxides and can be currently implemented in speciation codes.

Table 2
Parameters needed for NEM, CCM, DLM, and TLM computation

	NEM	CCM	DLM	TLM
Site density (mol kg^{-1})	✓	✓	✓	✓
Surface area (m^2 g^{-1})		✓	✓	✓
Site protolysis constants	✓	✓	✓	✓
Me sorption constants	✓	✓	✓	✓
Me sorption planes				✓
Capacitance(s)		✓		✓
		(1 parameter)		(2 parameters)

All of the cited models were able to reproduce successfully sorption data on montmorillonite, although they did not consider the same hypotheses. It should also be noticed that all but one of them (the NEM) were applied to only one set of data without any attempt to reproduce data from other sources. Moreover, electrostatic model parameters were rather loosely constrained. For instance, some authors derived their electrostatic model and related parameters from only one titration curve obtained at a single ionic strength (Stadler and Schindler, 1993; Ikhsan and others, 2005; Bogolepov, 2009). In some other studies, edge surface properties are described to be equivalent to a mix between silica (quartz or amorphous silica) and alumina (gibbsite) surfaces without any further comparison to experimental titration data (for example, Zachara and Smith, 1994). Consequently, these models must be evaluated in the following section in terms of representativeness of their hypotheses with regard to what is known about montmorillonite surface properties and metal speciation on these surfaces. Accordingly, the next section depicts the pre-requisites for an "ideal" mechanistic model for pH dependent specific sorption on montmorillonite edge surfaces.

Prerequisites for an "ideal" mechanistic model for pH dependent specific sorption on montmorillonite edge surfaces

Overview of the Section

In this section, we discuss the parameters that are necessary for the development of a surface complexation model for montmorillonite edge surfaces, that is, (i) the surface potential and the related parameters given in table 2, (ii) the protonation/deprotonation constants for each reaction site and (iii) the reaction stoichiometries for divalent metal surface complexation. Specificities of montmorillonite are highlighted as well as unresolved issues.

A Representative Surface Area

The surface area is mandatory to calculate the surface potential as a function of pH for electrostatic models. It can also be used to constrain the amount of reactive sites based on crystallographic considerations. It has been emphasized in the first section that cations can sorb at different crystallographic positions (basal, interlayer and edge surfaces) and that surface complexation occurs only on edge surfaces. Logically, only the edge surface area should be considered for modeling surface complexation on montmorillonite edges, which is not the case in many studies (for example, Stadler and Schindler, 1993; Barbier and others, 2000; Ikhsan and others, 2005; Marcussen and

Table 3

Edge and basal specific surface areas for montmorillonite according to AFM and DIS measurements. Total (using ethylene glycol adsorption measurements) and BET specific surface area are given for comparison when available.

Studies	Methods	Sample	Specific surface area (m^2 g^{-1})			
			Edge	Basal	Total	BET
Tournassat and others, 2003	AFM and DIS	MX80 (< 2μm, Na-form)	8.5	26.6		31.4[a]
Yokoyama and others, 2005	AFM	Kunipia-P (Na-form)	5.3			7.7-21.3
Duc and others, 2005b	DIS	Swy-2 (< 2μm, Na-form)	19.2			
Perronnet and others, 2007	DIS	Prassa (< 20μm, Na-form)	25	67.5		102
		OrduArtikli (< 20μm, Na-form)	29.8	51.2		101
Le Forestier and others, 2010	DIS	Swy-2 (< 2μm, Na-form)	25.4	21.7	736.8	45.4
		Synthetic montmorillonite	22.7	62.8	763.8	87.1

[a] Value from Wanner and others (1994).

others, 2009; Gu and others, 2010). The main reason is that many authors measure the specific surface area with the Brunauer-Emmett-Teller (BET) technique. They apply it to their surface complexation models without considering that BET does not probe the reactive surface of interest, but the whole external surface of montmorillonite particles (that is, in case of a perfectly stacked particle, the edge surface of all TOT layers from the particles, plus at least the two exposed basal surfaces). This is dubious because (i) the measured areas cannot be relevant to dilute suspensions where TOT layers are almost completely dispersed (Sposito, 1992), given that BET measurements are performed on dry samples and (ii) outer montmorillonite basal surfaces are never negligible compared to edge surfaces. Two main techniques allow the measurement of montmorillonite specific edge surface area: (i) atomic force microscopy (AFM–Bickmore and others, 1999; Tournassat and others, 2003; Yokoyama and others, 2005) and (ii) low pressure gas adsorption using the Derivative Isotherm Summation (DIS) procedure (Villiéras and others, 1997; Tournassat and others, 2003; Perronnet and others, 2007; Le Forestier and others, 2010). Table 3 gives an overview of published montmorillonite specific surface area values obtained from AFM and DIS methods. When available, edge, basal (that is surface of particle aggregates minus edge surface) and total area are given. Specific edge surface area ranges from 5 to 30 m^2 g^{-1}. It demonstrates that results from BET measurements should not be used, since the surface probed is often as much as four times higher than the reactive edge surface. The use of BET surface area instead of edge surface area results in a drastic decrease in the surface charge density and so in the absolute value of the surface potential term. This problem is very specific to clay mineral surface reaction modeling and is a direct consequence of the presence of, at least, two types of reactive surfaces with very

different properties (edge and basal/interlayer surfaces), a feature that is not present in "classically" investigated oxides where BET area is often a good approximation for the reactive surface area.

A Reliable Surface Electrostatic Potential

Electrostatic surface potentials cannot be measured in aqueous solutions (Stumm and others, 1976) and must consequently originate from a model (Sposito, 2004). The various existing models for clays, depicted in figure 4, link the surface potential to the surface charge and the ionic strength. The surface charge is usually obtained from titration measurements, where the consumption or release of a proton by/from the surface is measured as a function of acid/base additions at various salt background concentrations (potentiometric measurements). If the initial charge of the titrated system is known, these measurements make it possible to obtain the point of zero net proton charge (p.z.n.p.c., where $\sigma_H = 0$ C m^{-2} is the net proton charge) by identifying the crossover point of two or more titration curves. In the case of solids with no structural charge ($\sigma_0 = 0$ C m^{-2}), the p.z.n.p.c. is equal to the point of zero net charge (p.z.n.c.) and the titration curve is directly related to the intrinsic charge of the surface (σ_{in}) (Sposito, 1998). Additional macroscopic information is usually acquired from the isoelectric point (i.e.p.) obtained by electrophoretic mobility measurements. A model is then constructed to reproduce all of these macroscopic measurements with the adjustable parameters listed in table 2. Structural information and data obtained from simulation at the molecular scale (for example molecular dynamics, density functional theory) can help to constrain these parameters. Even with "simple" systems, this procedure often fails to obtain a unique successful model for data description (Leroy and others, 2011). For montmorillonite surfaces, the task is even more difficult:

(i) Titration curves do not exhibit any crossover point due to the presence of a permanent structural charge (Duc and others, 2005a). The p.z.n.p.c. cannot be determined with this method. Moreover, the permanent structural charge is ten times higher than the variable proton charge and thus the electrophoretic mobility is largely dominated by the properties of basal surfaces; for this reason, montmorillonite has neither isoelectric point nor p.z.n.c. in the [1-13] pH domain.
(ii) Titration curves are highly sensitive to the pre-conditioning of the clay and to the measurement procedure (Duc and others, 2005b). This makes the calibration of a model very difficult, since there is a large uncertainty regarding the titration data values.
(iii) The models illustrated in figure 4 were initially developed for metal or oxide surfaces with the underlying hypothesis that the charge is homogeneously distributed on a flat and infinite surface. For montmorillonite surfaces, this is not the case: permanent structural charge is distributed on the basal surfaces while variable charge is localized on the edges (see fig. 1).

Several authors have attempted to tackle the problem corresponding to point (iii). Secor and Radke (1985) and Chang and Sposito (1994, 1996) studied the interplay of permanent charge and edge charge on the electrostatic potential developing at the edge surface. They demonstrated that the permanent negative potential at the basal surface may spill over to dominate a positively charged edge surface at low electrolyte concentrations and that the spill-over effect diminishes with an increase in electrolyte concentration. Kraepiel and others (1998, 1999) represented the clay particle as a semi-infinite homogeneous porous solid immersed in an aqueous solution. In this representation, the distribution of permanent charges is smeared over the layers and interlayers instead of being localized on the layers. More recently, Bourg

and others (2007) were able to reproduce best available titration curves by solving the two dimensional Poisson-Boltzmann equation and by adjusting protonation/deprotonation constants of four functional surface groups whose surface densities were obtained from crystallographic considerations. The authors considered a diffuse layer model in a geometry in which TOT layers were completely dispersed in suspension (no stacking), thus corresponding to a dilute suspension of montmorillonite in a Li or Na salt background (Sposito, 1992). They also gave a calculation procedure to tackle the problem of point (i) where the titration curve is corrected from the initial charge of the clay suspension by means of an iterative procedure, provided that the exact pre-conditioning of the clay is known, a condition that is seldom fulfilled. Within this model and considering a montmorillonite permanent charge of -0.109 C m^{-2}, the edge surface potential (Ψ_{edge}) is related to the edge charge (Q_{edge}) through the following empirical expression:

$$\frac{F\Psi_{edge}}{RT} = A_1 \operatorname{asinh}[A_2(Q_{edge} + A_3)] \tag{11}$$

where $A_1 = 1.4 - 1.3 \log I$, and $A_2 = 11 + \log I$ and $A_3 = -0.02 \times (-\log I)^{1.46}$. The considered geometry is depicted in figure 5. Calculations have been performed in a box with a maximum distance from the basal surface $z_{max} = 18.3$ nm and a maximum distance from the edge $x_{max} = 15.2$ nm, together with a zero potential boundary condition for these two limits. At I = 0.001, z_{max} and x_{max} are lower than two Debye lengths (19.2 nm) and the potential calculation is thus strongly truncated. We re-performed these calculations by considering $z_{max} = x_{max} = 50$ nm, that is more than five Debye lengths for the lowest considered ionic strength (0.001) in order to avoid a truncation effect. Moreover, we considered symmetry boundary conditions at z_{max} and x_{max}. Our calculations (fig. 5) show that the approximation made in Bourg and others (2007) has little effect on the calculated potential at high ionic strength (0.1), where the potential truncation is low (two Debye lengths = 1.92 nm $\ll z_{max}$) and is more pronounced at low ionic strength (0.001) where the potential truncation is large (2 Debye lengths = 19.2 nm $\sim z_{max}$). Equation (11) is efficient in predicting the edge potential as a function of edge charge but a slightly better agreement between our predictions and equation (11) can be achieved by changing A_1, A_2 and A_3 to the following values: $A_1 = 1.4 - 1.2 \log I$, and $A_2 = 11 + \log I$ and $A_3 = -0.02 \times (-\log I)^{1.60}$.

Clay TOT layers are almost completely dispersed in dilute suspension with NaCl solute background but they can stack to form particles containing up to 10 to 20 TOT layers at high ionic strength, compaction and/or with different salt backgrounds (Schramm and Kwak, 1982). We investigated the effect of the spatial arrangement of TOT layers on the edge potential with two idealized cases: (i) an infinite and regular stacking of TOT layers with a perfect alignment of edge surfaces and (ii) a stack of only two platelets without alignment of edge surfaces. An infinite and regular stacking of TOT layers can be modeled using the same geometry as described above for the isolated TOT layer by setting the z_{max} value to half of the desired interlayer distance, taken here at 0.94 nm, that is an interlayer space made of three water layers. For I = 0.1 and 0.01, the edge potential of the stacked arrangement and of an isolated lamella are comparable (fig. 5). For I = 0.001, there is almost no effect of stacking for negative edge charge but there is a significant effect for positive edge charge. The effect of stacking is more pronounced when edge surfaces are not perfectly aligned: while the stacking effect is negligible at I = 0.1, the edge potential is systematically and significantly lower in that configuration than in the dispersed configuration for I = 0.01 and I = 0.001. Other spatial arrangements could also be tested. In particular, as a function of pH and ionic strength, TOT layers or particles can form edge-to-face

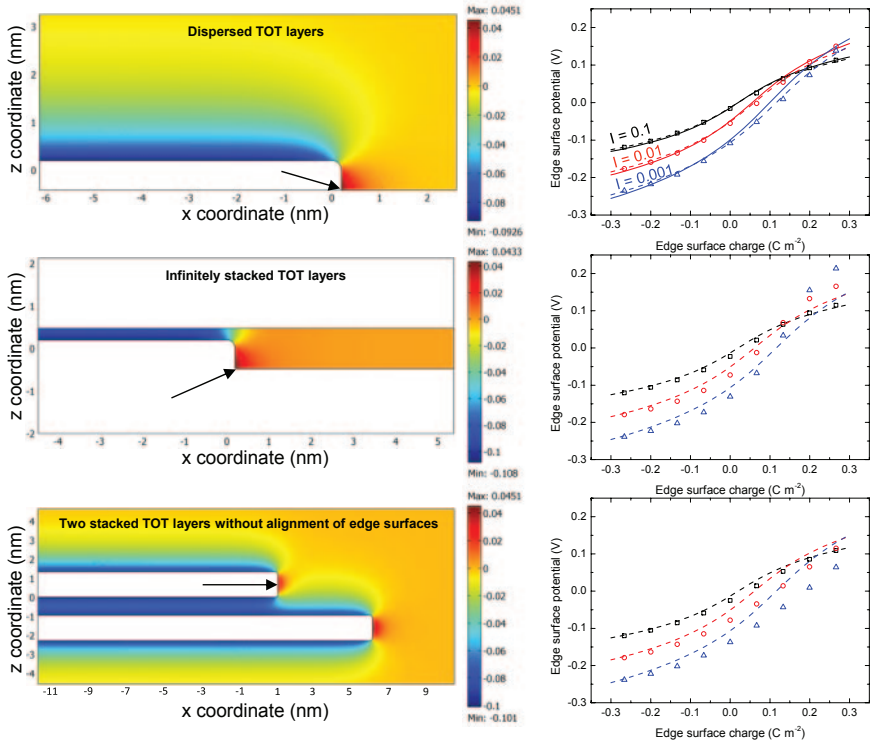

Fig. 5. Left: 2D geometry considered for solving the Poisson-Boltzmann equation (zoom on the edge surface region) in three different geometries. Top figure: dispersed platelets; middle figure: infinitely stacked platelets; bottom figure: two stacked platelets without alignment of edge surfaces along the x-axis. The color scale corresponds to the potential value (in V) for a uniform basal charge of -0.109 C m^{-2} and an edge charge of 0.1 C m^{-2} at an ionic strength of 0.1. The arrow indicates the center of the edge along the z-axis where the potential is plotted as a function of the edge charge in the right part of the figure. Right: edge potential as a function of edge charge for three ionic strengths (0.001, 0.01, and 0.1). Open symbols: results from calculations. Lines correspond to the empirical formula given in equation (11) with parameters from Bourg and others (2007) (plain lines) or from the present study (dashed lines).

hetero-coagulated assemblies (Tombacz and Szekeres, 2004) where negatively charged basal surfaces can interact with positively charged edge surfaces.

According to the above discussion, the estimation of a reliable surface potential as a function of surface charge is difficult for montmorillonite edges because of the large uncertainty regarding the particles' spatial arrangement. At least the model from Bourg and others (2007) seems to appropriately estimate the edge potential at I = 0.1, where little effect of the spatial arrangement on the potential was found (fig. 5). Figure 6 compares the relationships between the edge surface potential at I = 0.1, obtained with this model and other potential models conventionally used for surface complexation models (CCM and DLM, see fig. 4). Clearly, none of these "conventional" models is able to reproduce the peculiar relationship found for the montmorillonite edges. In particular, all of these models predict a zero potential for an edge charge of zero. This is clearly in disagreement with the spill-over effect of basal surfaces over edge surfaces. Consequently, electrostatic surface complexation models using these surface potential models should not be seen as more mechanistic than a non-electrostatic model. Delhorme and others (2010) went even further in their criticism of surface complexation models for clays. They performed Monte Carlo titration simulations in a

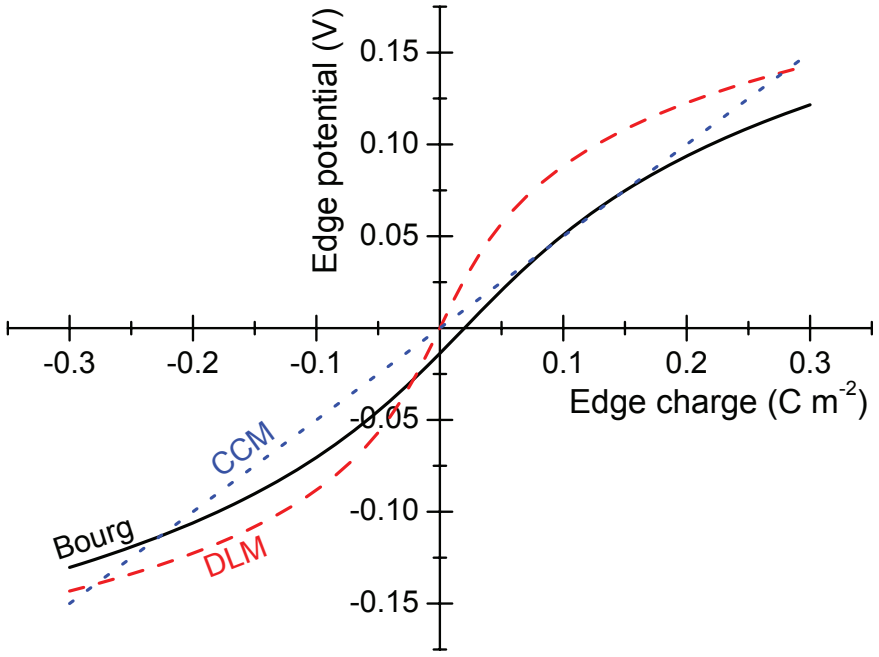

Fig. 6. Edge charge/edge potential relationship according to CCM (with a capacitance value of 2 F m^{-2}, dotted line), DLM (dashed line) and model from Bourg and others (2007, solid line) at I = 0.1.

geometry similar to that explored by Bourg and others (2007) and demonstrated that the mean field approximation is inappropriate to reproduce correctly the acid-base properties of their aluminol sites because of the discrete nature of titrating surface sites. This statement is unfortunately based on a rapid description of the differences between the two surface potential model outcomes rather than on a real quantification of the deviation as a function of experimental conditions. The largest discrepancies were observed in non-physical domains, namely the domain where 10^{-pH} exceeds their ionic strength values. The authors did not test either if it was possible to reduce the remaining discrepancy in physically correct domains by slightly changing the protonation/deprotonation constants in order to compensate the mean field approximation.

Constrained Values for Sorption Site Densities, Protonation/Deprotonation Constants and Reaction Stoichiometries

Sorption site densities are usually obtained from (i) potentiometric titration curve fitting (for example, Stadler and Schindler, 1993; Bradbury and Baeyens, 1997b; Ikhsan and others, 2005; Gu and others, 2010) and/or (ii) structural/geometrical considerations combined with specific surface area determination (for example, Zachara and Smith, 1994). The first method also makes it possible to obtain the protonation/deprotonation constants during the same fitting procedure. It also implies that all sites (or subset of sites) reactive with H^+ are also reactive with the considered divalent metal cation according to reaction 1. HES only represent a minor subset of the total sites (1-2 mmol kg^{-1}). Given the uncertainty on titration data (>1 mmol kg^{-1} on each point) and titration models emphasized in the previous paragraph, the determination of density and protonation/deprotonation constants from potentiometric titrations is impossible for HES. This method is thus relevant for LES

only. The second method is based on knowledge of the specific site density gained from crystallographic considerations (White and Zelazny, 1988). Site protonation/deprotonation constants can be obtained independently from two types of approaches: (i) either by fixing them at the values usually considered for simple constitutive oxides, namely silica and alumina (Zachara and Smith, 1994) or (ii) by calculating them from either a bond-valence model (Avena and others, 2003; Bickmore and others, 2003; Tournassat and others, 2004a) or from molecular simulations (for example, Churakov, 2006; Tazi and others, 2012). Until recently, none of these methods gave reliable pK_a values as demonstrated by Bourg and others (2007) and Delhorme and others (2010). However, Tazi and others (2012) could obtain recently relevant pK_a values for some of the sites present on the edges by taking into account natural electronic polarization effects. Although these approaches are promising, the determination of protonation/deprotonation constants currently relies on potentiometric titration data fitting because pK_a values obtained from atomistic simulations must be themselves compared with measurements. Moreover, not all the types of sites present on clay edges are usually investigated. For instance, model structures usually contain only Al and Si cations because these structures are derived from a pyrophyllite structure that is chemically different from montmorillonite, containing at least Mg and Fe in its octahedral sheet. As a direct consequence, pK_a of HES could not be predicted with the present state of the art even if their exact crystallographic configurations were known.

The same remarks also apply for the determination of the true stoichiometry of the reactions. Almost all modeling studies consider the "one site/one H^+/one Me^{2+}" stoichiometry given in reaction 1, with, if appropriate, additional contributions from hydroxylated species (Stadler and Schindler, 1993; Zachara and Smith, 1994; Bradbury and Baeyens, 2005b; Ikhsan and others, 2005; Gu and others, 2010):

$$>SOH + Me^{2+} + H_2O \rightleftharpoons SOMeOH + 2H^+ \qquad \text{Reaction 3}$$

$$>SOH + Me^{2+} + 2H_2O \rightleftharpoons SOMe(OH)_2^- + 3H^+ \qquad \text{Reaction 4}$$

The exact H^+/Me^{2+} stoichiometry can be obtained, in theory, from a comparison between potentiometric measurements in the presence and in the absence of added Me^{2+}. This type of experiment is seldom reported (Charlet and others, 1993; Ikhsan and others, 2005). In these two cases, the $H^+/Me^{2+/3+}$ stoichiometry differs from unity. This method is also restricted to the characterization of LES for the same reason as explained above: HES are not present in sufficient amounts to be probed by this method.

Implications

The above paragraphs highlight experimental and theoretical difficulties for obtaining reliable parameters in the framework of a mechanistic surface complexation model in the mean field theory approach. Some of these parameters cannot be constrained from available data but could be obtained with additional experimental work using currently available techniques (for example surface area, H^+/Me^{2+} stoichiometry for LES). Others cannot, such as reaction stoichiometry or pK_a for HES. These are necessarily *a priori* or fitting parameters. Additional spectroscopic work and molecular scale simulations are needed to overcome these problems.

Very little information is available for high energy site properties. Contrastingly, most low energy site properties can be probed experimentally and constrained by crystallographic considerations and molecular simulations. Linking the two sorption processes in a single model with the same underlying hypotheses and mechanisms is thus not supported by available data. Table 4 summarizes the requirements for the

TABLE 4

Summary of requirements and proposed guidelines for edge surface complexation model and parameters selection

Model / Parameters	Availability	Need	Avoid
Edge surface potential model (ψ) as a function of edge charge and ionic strength	Yes	Taking into account interplay of permanent charge and edge charge on the electrostatic potential developing at the edge surface	Using surface potential models developed for oxides and hydroxides
Edge specific surface area	Yes	AFM or DIS measurements	BET (or total) surface area
Surface site density for LES	Yes	Potentiometric titration curves and/or crystallographic considerations	
Protonation / deprotonation constants for LES	No	Fitting from potentiometric titration curves but the fitting parameters are not unique: it depends on the site attribution*	
Me/sites/H^+ stoichiometry for LES	No	Fitting or arbitrary values (could be constrained by potentiometric titrations performed with and without the presence of Me)	
Surface site density for HES	No**	Fitting or arbitrary values	
Protonation / deprotonation constants for HES	No	Fitting or arbitrary values	Considering these constants are the same as those for LES
Metal/sites/H^+ stoichiometry for HES	No	Fitting or arbitrary values	

* See Bourg and others (2007).

** Churakov and others (2012) proposed a method based on crystallographic considerations developed by comparison with Zn sorption data on Swy-1 montmorillonite. However, this promising method deserves further verifications using other metals and/or other montmorillonite materials.

building of a mechanistic surface complexation model for high and low energy sites, which were highlighted in this section.

CRITERIA FOR SORPTION DATA SELECTION, DATA REPRESENTATION, AND REMAINING EXPERIMENTAL OPEN ISSUES

Overview of the Section

In this section, we propose guidelines for selecting experimental conditions in order to calibrate a model for pH dependent specific sorption on high and low energy sites. Only data acquired at (25 ± 5) °C are considered. Firstly, the data selection made is based on the availability and on the relevance of experimental conditions. Secondly, we discuss why some of the selected data should be discarded for the calibration of a

surface complexation model, due to possible (surface) precipitation problems. Finally, we give some insights into unresolved issues that could prevent the interpretation of the data through a surface complexation model, that is, the reversibility problem and the effect of solid to liquid ratio.

Material Preparation and Control of Experimental Conditions

Composition of the equilibrium solution (salt background) and pH are needed for modeling cation exchange and pH dependent specific sorption. Some studies, often focused on engineering applications for heavy metal removal from polluted water, do not report both experimental conditions (table 5, "not suitable"). The procedure for starting material preparation is also of importance. A pure montmorillonite sample should be preferred to calibrate a mechanistic model since its use prevents, in principle, side mechanisms linked to the reactivity of other compounds present in the initial material [for example carbonate minerals, oxy(hydr)oxides and organic matter] or due to reagents added to the system (for instance, complexing organic compounds). At least twenty published studies report data obtained on a <2 μm fraction, but few of them applied additional treatments, such as acidification for carbonate removal, to prevent side mechanisms (table 5). Moreover, Me/clay ratio and the ionic strength conditions must be carefully selected to obtain data relevant for a given mechanism: cation exchange, high energy site sorption, low energy site sorption or surface (co-)precipitation (see second section). Briefly, HES can only be probed with experiments conducted at high ionic strength and for a metal/clay ratio of the order of 1 mmol kg^{-1} or below. A low metal/clay ratio is necessary to obtain a sorption behavior dominated by HES. A high ionic strength must be chosen for the same reason with regards to cation exchange: at low ionic strength cation exchange can dominate the retention mechanism, leading to a very weak dependence of the extent of retention with pH and consequently little information on HES reactivity. For pH <7.5, LES can be probed for metal clay loading as high as 50 mmol kg^{-1} without formation of metal pairs at the surface for Ni but not for Cu (40 mmol kg^{-1}, table 1). Above this value, precipitation occurs if silica is added to the suspension. The transition between LES sorption and precipitation dramatically changes if the pH value is raised to 8: Ni-Ni pairs can be observed for metal loading as low as 25 mmol kg^{-1} and neoformation of phyllosilicate is evidenced for metal loading of 45 mmol kg^{-1}. The surface coverage condition considerably reduces the range of data for mechanistic surface complexation model calibration.

Tracer Solubility Limits and Thermodynamic Database Considerations

At high pH, divalent metals precipitate in oxide or hydroxide forms even at low concentrations. Data interpretation with an adsorption model therefore needs to be restricted to the pH domain where such precipitations do not occur. Data selected for Zn and Cd sorption at ionic strength equal to $\sim$0.1 fulfil this condition (figs. 7 and 8). Ni sorption data are more problematic. Ni aqueous speciation and solubility are ill-defined (Thoenen, 1999; Hummel and Curti, 2003). According to the uncertainty on log K values for theophrastite (given in table 1 of Hummel and Curti, 2003), sorption data at high pH are potentially blurred by hydroxide precipitation, even at trace Ni concentration. The same remark applies for sorption data at pH 8 with equilibrium Ni concentration higher than 10^{-6} mol L^{-1} (fig. 9). Moreover, a catalytic effect of clay surface on Ni precipitation kinetics is expected (Scheidegger and others, 1997; Dähn and others, 2002). Consequently, experimental points that are oversaturated with regards to the minimum solubility limit should be disregarded for Ni sorption model calibration since the contribution of precipitation cannot be reliably estimated. This problem of tracer solubility is little addressed in the literature. When it

TABLE 5

Experimental conditions of sorption data from the literature. Data are classified as a function of their suitability for the calibration of a montmorillonite surface complexation model.

Source of the data	Starting clay material	Impurities removal using particle size fractionation and/or acid treatment	Knowledge of pH	Knowledge of ionic background	Investigated divalent metal(s)	Metal / clay ratio (mmol kg^{-1})
Selected data						
Baeyens and Bradbury, 1997	Swy-1	✓	[3-10.5]	0.01, 0.03 and 0.1 M $NaClO_4$	Zn, Ni	0.008-165 (HES and LES + cation exchange)
Bradbury and Baeyens, 1999	Swy-1	✓	[3-10]	0.0033 and 0.033 M $Ca(NO_3)_2$	Zn, Ni	<0.03-55 (HES and LES + cation exchange)
Selected data with few data points and/or small range of experimental conditions						
Tiller and Hodgson, 1960	Montmorillonite H25 from American Petroleum Institute Project No. 49	✓	[4-7]	0.1 M $CaCl_2$	Co, Zn	0.4 (Co) 0.7 (Zn) (HES)
Hodgson, 1960	Wyoming Bentonite	✓	[4-7]	0.1 M $CaCl_2$	Co	0.7 (HES)
Garcia-Miragaya and Page, 1976	Upton montmorillonite	✓	6.75 ± 0.25	0.01, 0.03, 0.05 and 0.17 M $NaClO_4$	Cd	0.06-0.5 (HES + cation exchange)
Stadler and Schindler, 1993	Swy-1	✓	[3.5-8]	0.1 M $CaClO_4$	Cu	10-50 (LES)
Zachara and others, 1993	Swy-1	✓	[4.6-8.5]	0.014 and 0.1 M $NaClO_4$ 0.001 M $Ca(ClO_4)_2$ and Na/Ca salt backgrounds	Cd	1.5 (HES + cation exchange)
Lothenbach and others, 1997	Swy-1	✓	[5-8]	0.1 M $NaNO_3$	Ni, Cu, Cd, Pb, Zn	50 (LES)
Lothenbach and others, 1999	Swy-1	✓	[5-8]	0.1 M $NaNO_3$	Cd, Zn	50 (LES)

TABLE 5
(continued)

Source of the data	Starting clay material	Impurities removal using particle size fractionation and/or acid treatment	Knowledge of pH	Knowledge of ionic background	Investigated divalent metal(s)	Metal / clay ratio (mmol kg^{-1})
Selected data with few data points and/or small range of experimental conditions						
Green-Pedersen and others, 1997	Na-bentonite (probably Swy-1 or Swy-2)	×	[7-8]	0.001 M $NaNO_3$	Ni	0.6-25 (dominated by cation exchange)
Green-Pedersen and Pind, 2000	Crook County montmorillonite (probably Swy-1 or Swy-2)	×	8	0.001 M $NaNO_3$	Ni	12-150 (dominated by cation exchange)
Morton and others, 2001	Cheto montmorillonite	✓	[2.5-11.5]	0.02 and 0.1 M $NaNO_3$	Cu	10-300 (LES + cation exchange + surface precipitation)
Tertre, 2005, Tertre and others, 2005	MX80 bentonite	✓	[2.5-9.5]	0.025 and 0.5 M $NaClO_4$	Ni	0.7 (HES + cation exchange)
Ikhsan and others, 2005	Swy-2	×	[4-10]	0.01 M KNO_3 and 0.0033 M $Ca(NO_3)_2$	Zn	32 (LES + cation exchange)
Bogolepov, 2009	Natural montmorillonite from Cherkassy deposit	×✓¥	[3.5-9]	0.01 and 0.1 M $NaClO_4$	Co	50 (LES + cation exchange)
Marcussen and others, 2009	Swy-2	✓	[4-7.5]	0.01 M $NaNO_3$	Ni	0.3-8.5 (HES and LES + cation exchange)
Dähn and others, 2011	STx-1 Milos montmorillonite	✓	7.1	0.1 M $NaClO_4$	Zn	2-40 (high and LES)

TABLE 5
(continued)

Source of the data	Starting clay material	Impurities removal using particle size fractionation and/or acid treatment	Knowledge of pH	Knowledge of ionic background	Investigated divalent metal(s)	Metal / clay ratio (mmol kg^{-1})
Suitable in principle but problematic						
Egozy, 1980 (**presence of acetate**)	Swy-1	✓	[5-6.5]	0.01, 0.02, 0.1, 0.3, 1 and 4 M NaCl / $NaNO_3$ + acetate	Cd, Co	~1-20 (HES and LES + cation exchange)
Di Toro and others, 1986 (**solid to liquid ratio effect due to cation exchange**[**])	Unknown from Wards Scientific	×	7-11	0.001 M of Na buffers	Ni	0.05-20 (HES and LES + cation exchange)
Gu and others, 2010 (**possible precipitation upon tracer addition**)	Upton montmorillonite	✓	[3-9]	0.001, 0.01, and 0.1 M $NaNO_3$	Ni, Cu, Cd, Pb, Zn	33 (LES + cation exchange + precipitation)
Ghayaza and others, 2011 (**presence of acetate**)	Swy-2	✓	5	0.04 M NaCl and $CaCl_2$ + acetate	Zn, Pb	0.1-100 (HES and LES + cation exchange)
Montavon and others, 2006 (**complex salt background + raw bentonite material**)	MX80 bentonite (in dispersed and compacted states)	×	[4-10]	Synthetic ground water (Na, K, Ca, Mg, etc.)	Ni	~0.1->1000 (HES and LES+ cation exchange)
Bradbury and Baeyens, 2011 (**complex salt background + raw bentonite material**)	MX80 bentonite	×	7.6	Synthetic ground water (Na, K, Ca, Mg, etc.)	Ni	0.001-25 (HES and LES+ cation exchange)

TABLE 5
(continued)

Source of the data	Starting clay material	Impurities removal using particle size fractionation and/or acid treatment	Knowledge of pH	Knowledge of ionic background	Investigated divalent metal(s)	Metal / clay ratio (mmol kg^{-1})
Not suitable						
Wold and Pickering, 1981	Montmorillonite from Polkville, Mississippi	✓	✓	✓	Pb	850 **(too high $[Me]_{tot}$)**
Barbier and others, 2000	Swy-2 and BASB	×	✓	✓	Pb, Cd	100-400 **(too high $[Me]_{tot}$)**
Ikhsan and others, 2005	STx-1	×	✓	✓	Zn	84 (STx-1) **(too high $[Me]_{tot}$)**
Tan and others, 2008, Xu and others, 2008b *	Lin'an montmorillonite	×	✓	✓	Ni	170 **(too high $[Me]_{tot}$)**
Xu and others, 2008a	MX80 bentonite	×	✓	✓	Pb	120 or 240 (edge) 60-160 (isotherm) **(too high $[Me]_{tot}$)**
Hu and others, 2009	MX80 bentonite	×	✓	✓	Ni	425 **(too high $[Me]_{tot}$)**
Yang and others, 2009	GMZ bentonite	×	✓	✓	Ni	204 (edge) 70-700 (isotherm) **(too high $[Me]_{tot}$)**
Song and others, 2009	Lin'an montmorillonite	×	✓	×✓§	Ni	167 **(too high $[Me]_{tot}$)**
Farrah and others, 1980	Montmorillonite from Polkville, Mississippi	✓	✓	×	Pb, Cu, Zn, Cd	250-500 **(too high $[Me]_{tot}$)**
Garcia-Miragaya and others, 1986	Upton montmorillonite	✓	✓	× **Salt background concentration is missing**	Cd, Zn	$5e^{-4}$ – 3.5

TABLE 5

(continued)

Source of the data	Starting clay material	Impurities removal using particle size fractionation and/or acid treatment	Knowledge of pH	Knowledge of ionic background	Investigated divalent metal(s)	Metal / clay ratio (mmol kg^{-1})
Not suitable						
Donat and others, 2005	Bentonite from Karakaya A.S. Mineral Company	×	✓	× **No information**	Ni, Pb	50-480 **(too high $[Me]_{tot}$)**
Sen Gupta and Bhattacharyya, 2008	Swy-2	×	✓	× **No information**	Ni, Pb, Cd	24-425 **(too high $[Me]_{tot}$)**
Kul and Koyuncu, 2010	Bentonite from Kütahya region (Turkey)	✓	× **No information**	× **No information**	Pb	241-1200 **(too high $[Me]_{tot}$)**

* Sorption data published in Tan and others (2008) and in Xu and others (2008b) are identical.

¥ Bogolopov (2009) states that the montmorillonite was separated from impurities, but no details are given, either on the method used or on the type of impurities removed. Impurities may consist of quartz and carbonates, including calcite (Fomina and Gadd, 2002).

§ Song and others (2009) used a montmorillonite after rinsing it with Milli-Q water until the conductivity of the washing solution reached that of pure water. They used 0.1 and 0.01 mol L^{-1} $NaClO_4$ for their experiments. However, their diffraction pattern is indicative of a Ca-saturated montmorillonite and the ionic salt background is certainly influenced by Ca desorbing from the clay. This could explain why they did not observe any significant difference between sorption edge at 0.1 and 0.01 mol L^{-1} $NaClO_4$.

** See text.

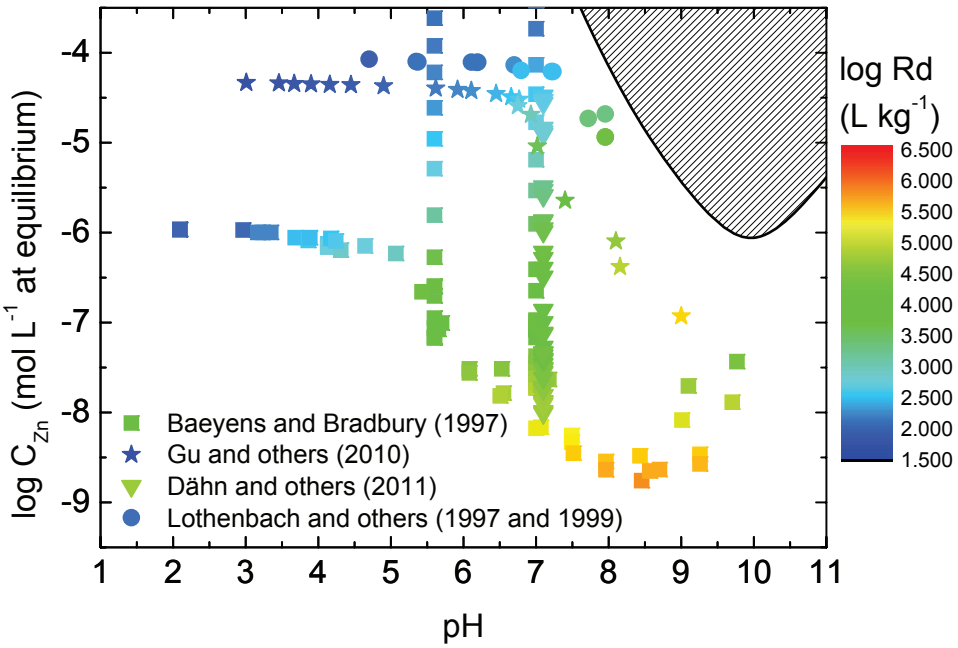

Fig. 7. Comparison of experimental Zn sorption data with Zn solubility limit at 0.1 ionic strength in Na salt background. Dashed domains (////) represent ZnO (zincite) precipitation domains according to the Thermoddem database (Blanc and others, 2012).

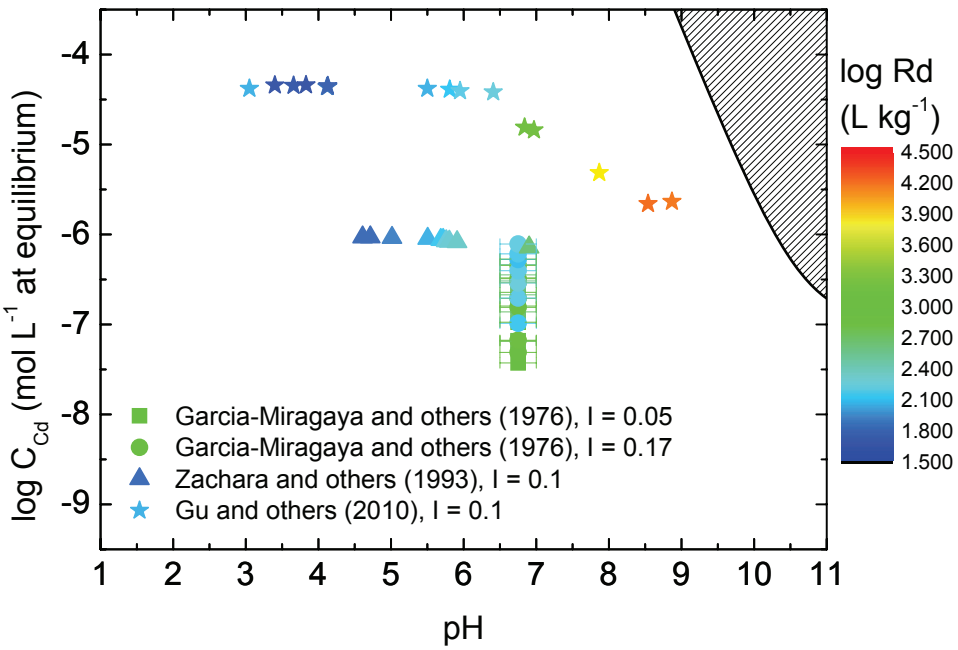

Fig. 8. Comparison of experimental Cd sorption data with Cd solubility limit at ~0.1 ionic strength in Na salt background. Dashed domains (////) represent $Cd(OH)_2$ precipitation domains according to the Thermoddem database (Blanc and others, 2012).

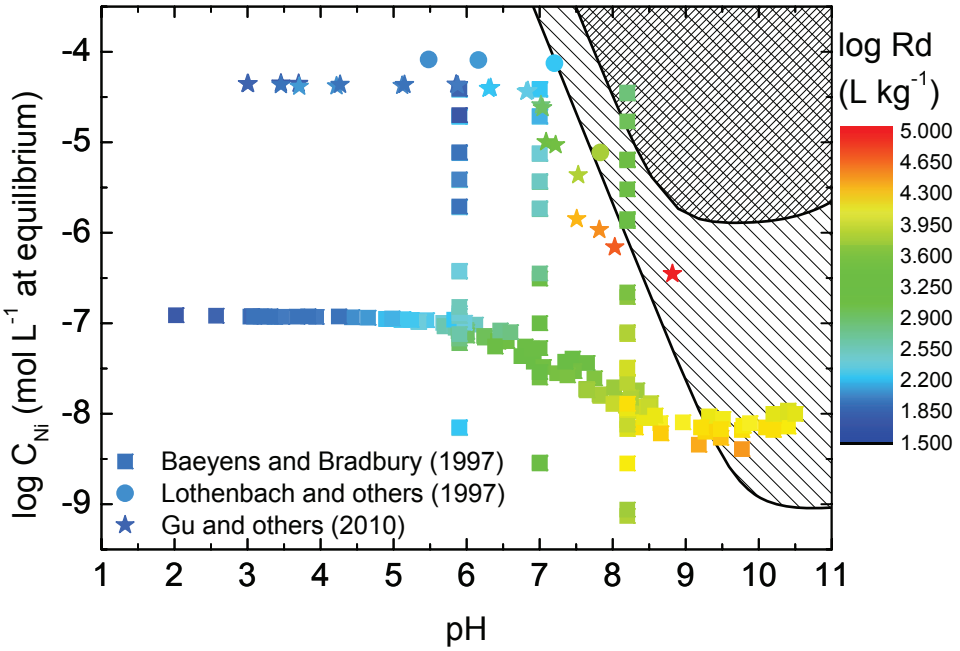

Fig. 9. Comparison of experimental Ni sorption data with Ni solubility limits at 0.1 ionic strength in Na salt background. Dashed domains represent $Ni(OH)_2$ (theophrastite) precipitation domains according to recommended log K and associated uncertainty by Hummel and Curti (2003): \\\\ = minimum solubility; //// = maximum solubility.

is considered, conflicting results are often available, as depicted by Appendix 2 for the Ni case.

Stability of the Sorbing Phase and its Surfaces

A strong but hidden hypothesis of sorption models is that the solid phase remains stable over the whole pH domain without alteration of the surface other than protonation/deprotonation and sorption processes. This is wrong: for instance, silica concentration increases significantly when pH is increased above 8.5 in a montmorillonite suspension (Tertre and others, 2005). Partial clay dissolution could alter sites such as HES that are present in small amounts at the clay surface. Spectroscopic investigations similar to those performed by Dähn and others (2011) performed at two pH values (for example 7 and 10) could probe if HES exist at high pH values. In the following, we will consider that the nature of the surface is not altered in the range of explored conditions (as in all currently reported clay sorption models), although there is no evidence for this.

Problematic Experimental Features for Mechanistic Surface Complexation Model Concepts

The reversibility problem.—Numerical sorption models based on surface complexation formalism make the assumption of fully reversible processes. To date, few studies have focused on the problem of clay sorption reversibility and the difficulty in data comparison is reinforced by the diversity in the cations tested and in the experimental conditions employed (pH, ionic strength, Me/clay ratio, *et cetera*). Table 6 gives an overview of available results on metal sorption reversibility. It indicates that distribution coefficients reported in the literature are not necessarily representative of

Table 6

Overview of results on metal sorption reversibility

	Reversibility / Irreversibility	Experimental conditions	Remark
Inskeep and Baham, 1983	Reversibility	Desorption by decreasing pH.	Experiments conducted at low ionic strength (I = 0.01).
Di Toro and others, 1986	Partial irreversibility	Desorption at constant pH by removing and replacing the supernatant solution.	Experiments conducted at low ionic strength (I = 0.01).
Hodgson, 1960	Partial irreversibility for interaction time above 3 days	Displacement of Co radiotracer by Cu, Zn or additional stable Co.	
Tiller and Hodgson, 1960	Partial irreversibility	Desorption by dilute acetic acid.	Irreversibly bound Co quantity increases with time.
Lothenbach and others, 1999	Reversibility after less than 4 weeks of reaction. Partial irreversibility after 60 weeks of interaction.	Acidification at pH 3.	Possible precipitation of $CdCO_3$ in long term experiments could explain the apparent irreversibility.
Baeyens and Bradbury, 1995	Tested but not shown		Part of retention seemed to be irreversible.
Morton and others, 2001	Partial irreversibility	Desorption by replacement of the supernatant solution by a Cu-free solution.	Part of irreversibility increase at high Me/clay ratio.

equilibrium between the solution and the surface and that some reversibility tests are more successful than others: for instance, decreasing the pH seems to be more efficient than decreasing Me concentration in the solution. If irreversibility could be further assessed and proven to contribute significantly to overall retention processes, the surface complexation approach could not help to model experimental results reliably. Fortunately, the irreversible part of sorption appears to be a very minor part of the overall sorption in the timescale explored by experimentalists. We will consider, as a working hypothesis, that specific sorption on clay edges is a reversible process.

Effect of solid to liquid ratio.—The influence of the solid to liquid ratio on the distribution ratio is a common issue in soil science. The distribution ratio is most often observed to decrease with the solid concentration. This phenomenon is called the "particle concentration effect" or "solid effect" (Limousin and others, 2007). Di Toro and others (1986) demonstrated this effect in the case of pure montmorillonite samples. After adding Ni radiotracer to a clay suspension sample, they measured the

remaining radiotracer concentration (C_a) in the supernatant after equilibration and centrifugation. Then, they removed part of the supernatant, re-suspended the solid, let it equilibrate, centrifuged it and again measured the remaining radiotracer concentration (C_{ra}). Surprisingly, $C_{ra} > C_a$ (by a factor ~1.2), meaning that Rd was lower in the final suspension than in the initial one. Thus, part of the radiotracer desorbed from the solid when the solid to liquid ratio (R_{SL}) increased, all other parameters being kept constant. At most the difference represented a decrease in the Rd value from 10,000 to 7,100 L kg^{-1} while R_{SL} increased from 0.1 g L^{-1} to 0.24 g L^{-1}. This difference in sorption could hardly be attributed to a kinetic problem because (i) the authors performed a control experiment and (ii) if so, sorption would have increased between measurement of C_a and C_{ra}. Inskeep and Baham (1983) also observed a "solid effect" for Cd sorption at I = 0.01 in $NaClO_4$. Interestingly the extent of the "solid effect" decreases with increasing ionic strength (Di Toro and others, 1986). This is in agreement with the results of Baeyens and Bradbury (1997) who noticed no difference for Ni sorption at I = 0.01 between R_{SL} of 0.24 (used for pH sorption edges) and R_{SL} of 1.1 g L^{-1} (used for concentration isotherms). Consequently, we must conclude that a "solid effect" takes place in clay sorption experiments at least for ionic strengths below 0.01 in sodium salt background and in suspension conditions. Only one study is available at high R_{SL} values that are representative of compacted systems: in Montavon and others (2006), the Ni Rd at pH > 7 decreased dramatically when R_{SL} increased from 10 g L^{-1} to 1000 g L^{-1} despite an ionic strength value higher than 0.01. A dependency of Rd value on R_{SL} would imply the necessity of using an activity coefficient correction for surface species that depends on the solid concentration in the suspension, as suggested by Voice and others (1983). To our knowledge, this type of approach has never been applied to surface complexation models for clay minerals. In the following, we will consider that there is no R_{SL} effect on the distribution coefficient for well-dispersed systems at ionic strengths above 0.01. However, this problem certainly merits further studies.

Effect of material source and heterogeneity.—At a given pH and given salt background concentration, the distribution coefficient should decrease as a function of increasing concentration due to the decrease in the relative contribution of HES on the overall sorption (fig. 3). Comparison of data points originating from different studies is problematic with regard to this aspect (fig. 10). For instance, Lothenbach and others (1997) and Baeyens and Bradbury (1997) obtained contrasting results even though they used the same starting material. The data point from Lothenbach and others, in figure 10, is at the limit of the $Ni(OH)_{2(s)}$ solubility domain according to the lowest solubility hypothesis (fig. 9). This data point could then be discarded due to a suspected additional (co-)precipitation process. The data point from Gu and others (2010) obtained on Upton montmorillonite is more problematic. It does not lie within the possible $Ni(OH)_{2(s)}$ solubility domain (fig. 9) and has a Rd value higher by one order of magnitude than corresponding data points from Baeyens and Bradbury (1997). Such a high Rd value cannot be explained by a data digitization error. Indeed, reducing Rd from ~5000 to ~4000 would mean that the percentage of Ni sorbed is not ~99 percent, as our data digitization indicates, but rather ~94 percent, which is far above the digitization error. Thus, this corresponds either to contrasted properties of Upton and Swy-1 montmorillonite surfaces or to experimental artefacts/differences leading to (co-)precipitation in Gu and others' experiments. Indeed, two experimental differences are notable. Firstly, Baeyens and Bradbury's experiments were carried out in a glove-box, preventing any artefact due to CO_2 solubilization in the system, which is not the case for Gu and others. The precipitation of a nickel carbonate phase could thus be suspected, but is actually irrelevant, because of the very high solubility product of the hydrated Ni carbonate phase [hellyerite, $NiCO_3(H_2O)_6$, Hummel and Curti,

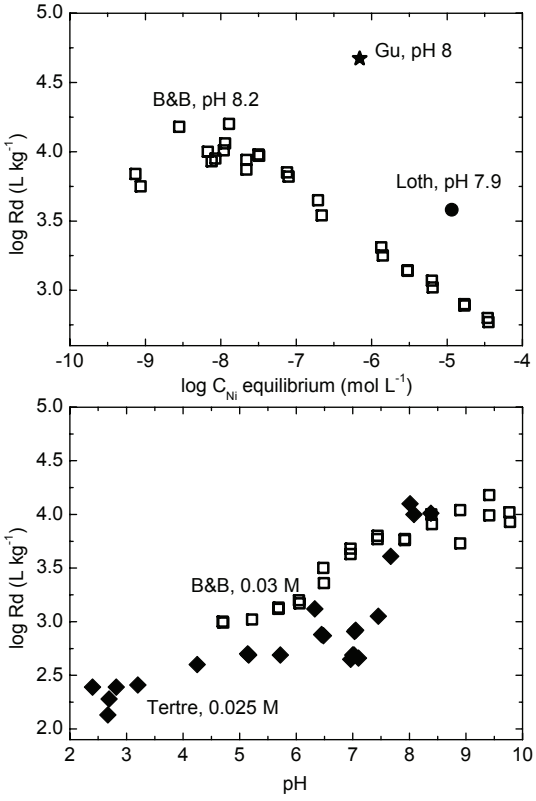

Fig. 10. Comparison of datasets for Ni retention on montmorillonite as a function of Ni equilibrium concentration at I = 0.1 and pH 7.9–8.2 (upper figure) or as a function of pH at I ~ 0.025–0.03 with trace concentration of Ni (bottom figure). Open squares: data from Baeyens and Bradbury (1997) obtained on Swy-1 montmorillonite. Black circle: data from Lothenbach and others (1997) obtained on Swy-1 montmorillonite. Black star: data from Gu and others (2010) obtained on Upton montmorillonite. Black diamonds: data from Tertre and others (2005) obtained on MX80 montmorillonite.

2003]. The second difference comes from Ni stock solution preparation and injection. Baeyens and Bradbury (1997) performed their sorption isotherm experiment by equilibrating a Ni solution at the desired pH and at constant salt background concentration. These solutions were labeled with a radiotracer and then added to the pre-equilibrated montmorillonite suspension. In contrast, Gu and others directly spiked 10 mL of montmorillonite suspension with 0.05 mL of Ni stock solution in order to reach a final metal concentration of 4.88 10^{-5} mol L^{-1}. This means that their spiking stock solution concentration was as high as 10^{-2} mol L^{-1}. This high concentration could have led to a rapid (co-)precipitation of Ni when entering into contact with the clay suspension at pH ~ 8, thus resulting in a very high final Rd value, because Ni precipitation would be irreversible at the timescale of the experiment. A similar problem could have been encountered in the study of Marcussen and others (2009) on Ni sorption at near neutral pH. Surprisingly, Zn sorption data from Ikhsan and others (2005) do not seem to suffer from the same problem even though their procedure of metal addition into the vessels was similar (stock solution at 0.01 mol L^{-1}). Additional data would be necessary to assess or discard this possible experimental artefact. Nonetheless, we decided to discard literature data exhibiting similar types of problems (see table 5).

Even at trace metal concentration, two different montmorillonite materials (MX80 and Swy-1), studied by two different research groups, have contrasting sorption behaviors: the Ni sorption edge of MX80 is shifted by more than one pH unit compared to that of Swy-1 (fig. 10). Although sample preparation did slightly differ in the two experiments [Tertre and others (2005) discarded the >0.5 μm clay fraction while Baeyens and Bradbury (1997) did not], this difference in reactivity amongst clay samples cannot be ignored when calibrating and comparing sorption models.

Data Uncertainties and Pitfalls in Data Representation

Error calculation is crucial for data/model comparisons. However, the estimation of uncertainties associated with published sorption data is tricky, since the methods used for calculation are often not disclosed by authors and information relative to uncertainties associated with each step of the experimental procedure is scarce. If estimated, the uncertainty is often reported as an error band having a symmetrical and/or constant extent, whatever the experimental conditions and sorption results. However, error bands should be asymmetrical when the y-axis is in log scale, and error propagation calculation indicates that experimental points at high sorption values should have lower relative uncertainty than experimental points at low sorption values. Appendix 3 gives some insights into this problem, taking examples from the literature.

Implications

Table 7 summarizes identified requirements for data selection and highlights problems linked to their interpretation with a surface complexation model. Some of them are obvious but are not always respected. A selection of data is proposed in table 5 according to the criteria given in this section. Accordingly:

(i) There is little relevant data available in the literature. Only two studies (coming from the same team of scientists) are sufficiently precise and complete to probe sorption on HES, LES and cation exchange. Other studies often focus on a narrow range of pH or Me/clay ratios or on a single ionic strength condition.
(ii) A larger set of data is available for sorption concerning HES (metal to clay ratio of the order of 1 mmol kg^{-1} or less) than for LES.

SURFACE COMPLEXATION MODELS FOR DIVALENT METAL SORPTION ON MONTMORILLONITE SURFACES

Methodology

Most of the available data can only be used to constrain HES reactivity and cation exchange. There is far less data to constrain LES reactivity. Therefore, model development for HES is presented first. HES properties are very ill-defined and are mostly fitting parameters. Consequently, we first apply the method referred to as Ockham's Razor (or the rule of parsimony), which states that, when choosing among rival hypotheses, all of which explain the observed facts, the simplest is preferred (McBride, 1997). The first modeling approach explored in this section is thus a "minimalist" modeling approach, which attempts to minimize the number of adjustable parameters for modeling the largest number of sorption data on HES. In so doing, we show that a surface complexation electrostatic model is not efficient at reproducing the data although it should represent more correctly the physical nature of the metal/clay surface interactions. Then, an alternative electrostatic sorption model is proposed in an attempt to solve this problem. Finally, we show that an electrostatic model can be used successfully for LES modeling.

Table 7

Overview of experimental requirements for data selection and interpretation by a surface complexation model. Some guidelines are given for future data acquisition

	Requirements	**Additional remarks**
Data representation	In most cases, Rd representation must be preferred to % representation. Data uncertainties and their estimation/calculation method should be provided.	
pH	Plots of Me sorption as a function of pH over a wide pH range (3-10) are necessary.	Ideally, it would be necessary to check changes in the nature of surface sites at high and low pH (is there site disappearance – or appearance – due to edge surface dissolution?).
Ionic strengths	High ionic strengths are necessary to probe the presence of high (and low) energy sites.	Salt background concentrations must be known for modelling purposes.
Sample preparation	Removal of non-clay minerals is required to avoid side effects from accessory mineral sorption or dissolution.	
Me concentration	Concentrations must be below solubility limits. Exploring a range of concentrations provides information on site densities.	Spiking the tracer from a concentrated solution must be avoided in order to prevent over-concentration effects and non-reversible rapid (co-) precipitation of the tracer upon introduction in the vessels.
Me/Clay ratio	The ratio must not exceed ~1 mol kg^{-1} for HES detection and ~30 mmol kg^{-1} for LES detection.	Above 30 mmol kg^{-1}, surface condensation and precipitation may occur that cannot be modelled by surface complexation models
Solid to liquid ratio	Rd values should not depend on R_{SL} if sorption site saturation is not attained (otherwise the dependence must be an increase in Rd with an increase in R_{SL}).	This requirement is not met at least for (i) low ionic strengths at low R_{SL} and (ii) high ionic strengths at high R_{SL}.
Montmorillonite samples	If a general model is desired (with possible extrapolation to other materials), the Rd values should not depend on the chosen montmorillonite sample.	Most of the available selected data were obtained on Swy-1. Data obtained on the MX80 montmorillonite fraction are different.
Reversibility	Sorption must be reversible for interpretation through surface complexation modelling.	

Building An Efficient Surface Complexation Model For HES. Why Are Non-Electrostatic Models So Successful?

Equations and constraints.—A generalized version of reaction 1 can be written:

$$>SOH_n + Me^{2+} \rightleftharpoons SOH_{n\text{-}x}Me^{2\text{-}x} + xH^+ \qquad \text{Reaction 5}$$

where n and x are positive integers and K_{Me}^{HES} is defined as an equilibrium constant according to:

$$K_{Me}^{HES} = \frac{[\rangle SOH_{n-x}Me^{2-x}]}{[\rangle SOH_n]} \frac{(H^+)^x}{(Me^{2+})} \exp\left(\frac{(2-x)F\Psi_0}{RT}\right). \qquad (12)$$

We assume here that only one site is responsible for the high energy site sorption behavior. In that case, and neglecting retention by cation exchange (that is, working at high ionic strength), it is possible to relate the measured Rd value to the concentration of sites occupied by Me, $[\rangle SOH_{n-x}Me^{2-x}]$:

$$Rd = \frac{[\rangle SOH_{n-x}Me^{2-x}]}{C_{Me}R_{SL}}. \qquad (13)$$

The activity of Me^{2+} in solution, (Me^{2+}), is related to the concentration of the free cation in solution, $[Me^{2+}]$, and its activity coefficient γ_{Me}: $(Me^{2+}) = \gamma_{div}\,[Me^{2+}]$. Divalent metal cations are hydrolysed as a function of pH and thus $[Me^{2+}]$ is not equal to C_{Me}. Neglecting Me^{2+} complexation by other solute species, it ensues that:

$$[Me^{2+}] + [MeOH^+] + [Me(OH)_2] = C_{Me} \qquad (14)$$

with $MeOH^+$ and $Me(OH)_2$ being formed with the following reaction:

$$Me^{2+} + H_2O \rightleftharpoons MeOH^+ + H^+ \qquad K_{MeOH} \qquad \text{Reaction 6}$$

$$MeOH^+ + H_2O \rightleftharpoons Me(OH)_2 + H^+ \qquad K_{Me(OH)2} \qquad \text{Reaction 7}$$

Combining equations (12) and (14):

$$\log Rd = x\,pH + \log\left(\frac{K_{Me}^{HES}{}_{Me}[\rangle SOH_n]}{R_{SL}\left(\frac{1}{\gamma_{Me}} + \frac{K_{MeOH}}{\gamma_{MeOH}10^{-pH}} + \frac{K_{Me(OH)_2}K_{MeOH}}{10^{-2pH}}\right)}\right) - \left(\frac{(2-x)F\Psi_0}{RT\ln 10}\right). \qquad (15)$$

The three terms of equation (15) are related to the pH: $x\,pH$ is linearly related to the pH; the second one depends on the terms related to Me speciation in solution, $\left(\frac{1}{\gamma_{Me}} + \frac{K_{MeOH}}{\gamma_{MeOH}10^{-pH}} + \frac{K_{Me(OH)_2}K_{MeOH}}{10^{-2pH}}\right)$, but also on the surface term $[\rangle SOH_n]$ because of the possible protonation and/or deprotonation of the sorbing site and Me sorption as a function of pH: $([\rangle S_T] = [\rangle SOH_{n-x}Me^{2-x}] + \sum_{j\geq 0} [\rangle SOH_j^{(j-n)+}]$, where $[\rangle S_T]$ is the total concentration of sites); finally, the third term, $-\left(\frac{(2-x)F\Psi_0}{RT\,ln\,10}\right)$ is related to the pH according to the relationships between the surface charge, and the surface potential, Ψ_0. Since HES represent only a very minor part of the total surface site concentration, the surface potential should not be influenced by Me sorption on the surface and is only dependent on ionic strength and pH. The slope of log Rd *versus* pH is equal to or less than one, for Zn, Ni and Cd sorption on HES (fig. 11). These elements are present

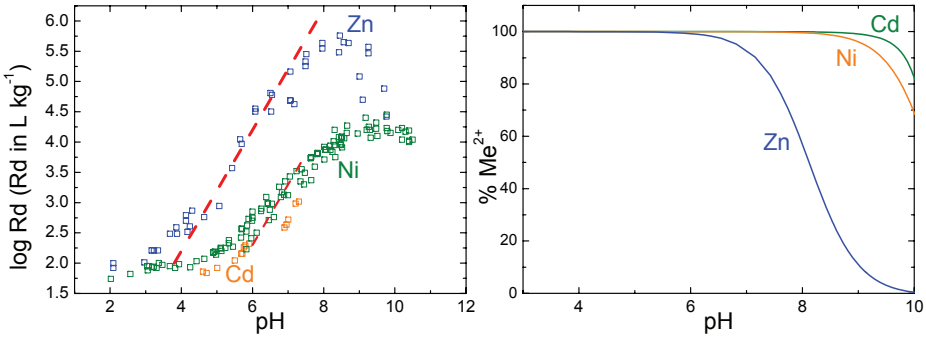

Fig. 11. Left figure: sorption edge for Zn, Ni (Baeyens and Bradury, 1997) and Cd (Zachara and others, 1993) on Na-montmorillonite at I = 0.1. Dashed red lines correspond to 1:1 log Rd/pH slopes. Right figure: relative abundance of the free divalent cation, Me^{2+}, in solution according to the Thermoddem database (http://thermoddem.brgm.fr/) for Zn and Cd and Hummel and Curti (2003) for Ni.

in their free Me^{2+} form in solution in the pH range of increasing sorption (pH ~3 to ~7). In these conditions, the simplest way to reproduce the observed slope is to consider a stoichiometry value x equal to 1 and to neglect the electrostatic term, leading to:

$$\log\ Rd = pH + \log\left(\frac{\gamma_{Me} K_{Me}^{HES}{}_{Me}[\rangle \mathrm{SOH_n}]}{R_{SL}}\right). \tag{16}$$

These modeling hypotheses, introduced by Bradbury and Baeyens (1997b), enabled these authors to model a large range of sorption data with a small number of adjustable parameters: sorption site density, association constant K_{Me}^{HES} for various elements and protonation/deprotonation constants for HES. The sorption site density was itself constrained by a change in the slope of log C_{sorb} *versus* log C_{eq} in sorption isotherms. The protonation/deprotonation properties of the HES were arbitrarily chosen at values identical to those of LES. Equation (16) implies that the linear part of the sorption edge must be obtained in the pH domain where $\log\left(\frac{\gamma_{Me} K_{Me}^{HES}{}_{Me}[\rangle \mathrm{SOH_n}]}{R_{SL}}\right)$ is almost constant, that is where $[\rangle \mathrm{SOH_n}] \approx [\rangle \mathrm{S_T}]$ (all other terms being constant). For this reason, the linear part of the Zn sorption edge between pH 4 and pH 7 implies that the deprotonation pK_a value must be, at least, greater than 7 and the protonation pK_a value must be lower than 4. The sorption edge levels off at pH values greater than 7. This is indicative either of a deprotonation of the sorption site and/or the hydrolysis of the metallic cation in solution following reaction 6 and reaction 7. The consideration of solute Me hydrolysis only is not sufficient to reproduce Zn sorption edge data (fig. 12) and site deprotonation is necessary. No additional parameter is needed to reproduce the data. With the approach described above, it is then possible to define a "minimalist" approach for the sorption of each divalent metallic cation, following Ockham's Razor rule.

Comparison with 2SPNE SC/CE Models (2 site protolysis non-electrostatic surface complexation and cation exchange model).—Bradbury and Baeyens (1997a) pointed out that the real modeling challenge is to find a minimal set of parameters that reproduces both sorption data for all divalent metallic cations in all tested conditions and the clay titration curve. However, HES properties are not constrained by titration data for site protonation/deprotonation constants. The only remaining challenge is thus to reproduce the sorption data set for various cations with a unique set of parameters for HES

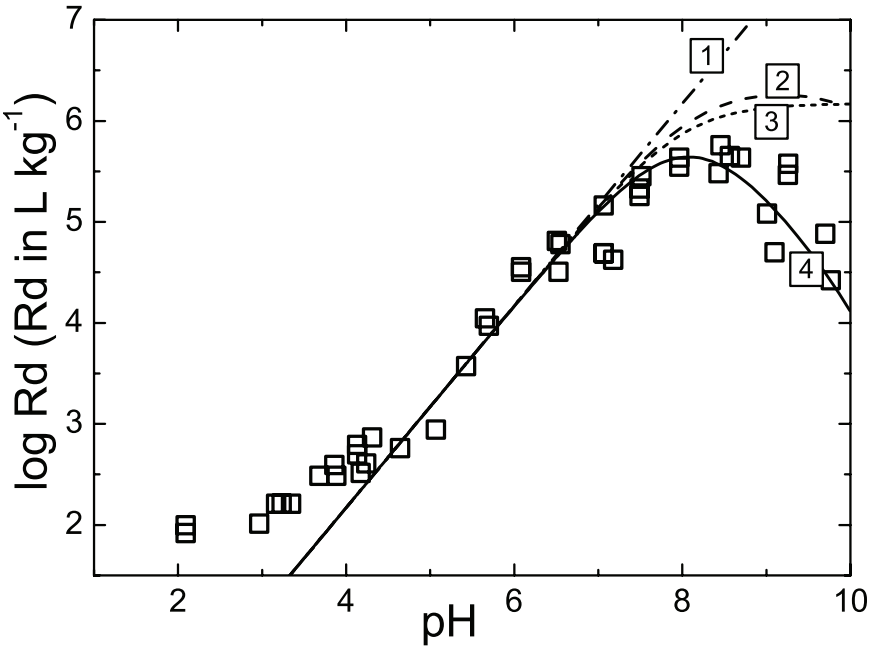

Fig. 12. Symbols: Zn sorption edge at I = 0.1 (data from Baeyens and Bradbury, 1997). Lines: models assuming: (1) only sorption reaction $\rangle SOH + Zn^{2+} \rightleftharpoons \rangle SOZn^{+} + H^{+}$, (2) sorption reaction and Me hydrolysis in solution $Zn^{2+} + H_2O \rightleftharpoons ZnOH^{+} + H^{+}$ and $ZnOH^{+} + H_2O \rightleftharpoons Zn(OH)_2 + H^{+}$, (3) sorption reaction and deprotonation of sorption site $\rangle SOH \rightleftharpoons \rangle SO^{-} + H^{+}$, and (4) all above processes taken into account.

properties. The underlying hypothesis is that all of these cations compete for the same type of site. Its validity was demonstrated experimentally with Co/Ni/Zn competition experiments (Bradbury and Baeyens, 2005a). Surprisingly, this competition was not considered in the revised 2SPNE SC/CE model (Bradbury and Baeyens, 2005b). Note that metals with dissimilar chemistries (for example different valence states, such as Co and Eu) do not compete: their high energy sorption sites are different and their site density, protonation/deprotonation constants might be different. The parameters of the two versions of Bradbury and Baeyens' models are summarized in table 8. For comparison, we fitted the same set of data as that used for 2SPNE SC/CE model calibration with the above described "minimalist" approach. We considered sorption competition with Zn and Mn, also present in the Swy-1 Na-montmorillonite. We also considered the uncertainty regarding the thermodynamic database for Ni data (fig. 13). Surface affinity constants of non-hydrolyzed species are very close to those of the 2SPNE SC/CE model. The fitted deprotonation constant for the high energy site is also close to the value for the weak site of the 2SPNE SC/CE model (however, this result must be seen as being fortuitous according to the analysis made in the previous section). Conversely, the site protonation constant and the surface affinity constants for the hydrolyzed species ($\rangle SOMeOH^{+}$ and $\rangle SOMe(OH)_2$) are not needed for data simulation. This means that some of the 2SPNE SC/CE parameters are unconstrained. This is especially true for sorption of Ni, Mn and Zn hydroxylated species (table 8).

Application to the available range of literature data.—The applicability of the minimalist approach was further tested with data covering a range of analytical conditions, such as the effect of ionic strength and the replacement of Na by Ca on Ni sorption, or the impact of pH and ionic strength on Cd sorption (figs. 14 and 15 and references

Table 8

Parameters for the two versions of the Na-montmorillonite non-electrostatic model from Bradbury and Baeyens (1997b and 2005b) and comparison with the proposed "minimalist" model calibrated with data obtained at I = 0.1 in $NaClO_4$ salt background (Ni and Zn: Baeyens and Bradbury, 1997; Cd: Zachara and others, 1993). HES density is 2 mmol kg^{-1} for the three models

Parameters	log K of the reactions		
	Bradbury and Baeyens' 1997 model*	Bradbury and Baeyens' 2005 model**	This study: "Minimalist" model*
HES protonation / deprotonation			
$>SOH + H^+ \rightleftharpoons >SOH_2^+$	4.5	4.5	Not necessary
$>SOH \rightleftharpoons >SO^- + H^+$	-7.9	-7.9	-8.3
Zn speciation			
$Zn^{2+} + H_2O \rightleftharpoons ZnOH^+ + H^+$	0.59	-8.96	-7.83‡‡
$Zn^{2+} + 2\ H_2O \rightleftharpoons Zn(OH)_2 + 2\ H^+$		-16.9	-17.9‡‡
$Zn^{2+} + 3\ H_2O \rightleftharpoons Zn(OH)_3^- + 3\ H^+$		-28.4	-27.7‡‡
$2\ NaX + Zn^{2+} \rightleftharpoons ZnX_2 + 2\ Na^+$	0.59	0.59	0.6
$>SOH + Zn^{2+} \rightleftharpoons >SOZn^+ + H^+$	1.6	1.6	1.5
$>SOH + Zn^{2+} + H_2O \rightleftharpoons >SOZnOH + 2\ H^+$	-	-7.4	Not necessary
$>SOH + Zn^{2+} + 2\ H_2O \rightleftharpoons >SOZn(OH)_2^+ + 3\ H^+$	-	-17	Not necessary
Mn speciation			
$Mn^{2+} + H_2O \rightleftharpoons MnOH^+ + H^+$	-10.6	-10.6	-10.6‡‡
$Mn^{2+} + 2\ H_2O \rightleftharpoons Mn(OH)_2 + 2\ H^+$	-	-22.2	-22.2‡‡
$Mn^{2+} + 3\ H_2O \rightleftharpoons Mn(OH)_3^- + 3\ H^+$	-	-	-34.8‡‡
$2\ NaX + Mn^{2+} \rightleftharpoons MnX_2 + 2\ Na^+$	-	-	0.3
$>SOH + Mn^{2+} \rightleftharpoons >SOMn^+ + H^+$	-0.2	-0.6	-0.4
$>SOH + Mn^{2+} + H_2O \rightleftharpoons >SOMnOH + 2\ H^+$	-	-11	Not necessary
Nickel speciation			
$Ni^{2+} + H_2O \rightleftharpoons NiOH^+ + H^+$	-9.5	-9.86	-9.14 to -9.86‡
$Ni^{2+} + 2\ H_2O \rightleftharpoons Ni(OH)_2 + 2\ H^+$	-18	-19	-16.4 to -19.4‡
$Ni^{2+} + 3\ H_2O \rightleftharpoons Ni(OH)_3^- + 3\ H^+$	-29.7	-30	-27.7 to -31.7‡
$2\ NaX + Ni^{2+} \rightleftharpoons NiX_2 + 2\ Na^+$	0.49	0.49	0.5
$>SOH + Ni^{2+} \rightleftharpoons >SONi^+ + H^+$	-0.1	-0.6	-0.2
$>SOH + Ni^{2+} + H_2O \rightleftharpoons >SONiOH + 2\ H^+$	-	-10	Too dependent on solute Ni speciation uncertainties

TABLE 8

(continued)

Parameters	log K of the reactions		
	Bradbury and Baeyens' 1997 model*	Bradbury and Baeyens' 2005 model**	This study: "Minimalist" model*
Nickel speciation (continued)			
$>SOH + Ni^{2+} + 2\ H_2O \rightleftharpoons >SONi(OH)_2^{+} + 3\ H^{+}$	-	-20	Too dependent on solute Ni speciation uncertainties
Cd speciation			
$Cd^{2+} + H_2O \rightleftharpoons CdOH^{+} + H^{+}$	-	-10.8	-10.1‡‡
$Cd^{2+} + 2\ H_2O \rightleftharpoons Cd(OH)_2 + 2\ H^{+}$	-	-20.35	-20.9‡‡
$Cd^{2+} + 3\ H_2O \rightleftharpoons Cd(OH)_3^{-} + 3\ H^{+}$	-	-	-33.3‡‡
$2\ NaX + Cd^{2+} \rightleftharpoons CdX_2 + 2\ Na^{+}$	-	0.3-0.45	0.4
$>SOH + Cd^{2+} \rightleftharpoons >SOCd^{+} + H^{+}$	-	-1	-0.5

* Assuming competition with natural Zn and Mn present in the Na-montmorillonite (Swy-1).
** Assuming no competition with natural Zn and Mn present in the Na-montmorillonite (Swy-1).
‡ From Hummel and Curti (2003).
‡‡ From the Thermoddem database (http://thermoddem.brgm.fr/).

therein). Ni sorption data from Baeyens and Bradbury (1997) are well predicted at low ionic strength in Na salt background (fig. 14). This result was expected according of the similarities between the 2SPNE-CE and the proposed approach. Results from Tertre and others (2005) are not so well reproduced (fig. 15A). These authors studied Ni sorption on a different clay material than Swy-1, namely a montmorillonite originating from MX80 bentonite. From the low pH part of the curve, the Ni exchange selectivity coefficient might be lower for MX80 than for Swy-1. The variability of cation exchange selectivity coefficients for various montmorillonite materials is assessed by data available from the literature, and the fitted selectivity coefficient value (-0.4 in $\log_{10}$ scale) is in agreement with the value found for Na-Ca exchange data obtained by Tournassat and others (2011) on the same material at low Ca surface loading. The sorption edge is well described at $I = 0.025$ if the corrected selectivity coefficient is considered (not shown), but the prediction at $I = 0.5$ remains inaccurate with a pH shift of more than one pH unit. This could be due either to (i) an absence of high energy sorption sites on MX80, (ii) a saturation of these sites by competing cations in greater amounts than in Swy-1 or (iii) a difference in affinity for these sites between MX80 and Swy-1. The last two hypotheses are not mutually exclusive. There is not enough available data to conclude about the exact reason for the observed discrepancy. For Cd, results from Zachara and others (1993) are very well predicted (fig. 15B). Surprisingly, results from Inskeep and Baham (1983) are not well predicted although their clay material was the same as in Zachara and others (1993) and the preparation procedures were similar (fig. 15C). Their reported ionic strength conditions might be in error: they prepared their vials by mixing ten milliliters of dilute $Cd(ClO_4)$, 0.02 mol L^{-1} in $NaClO_4$ with a given volume of their 10 g L^{-1}, 0.01 mol L^{-1} in $NaClO_4$ clay stock suspension in order to obtain a final solid concentration of 2 g L^{-1} and an ionic

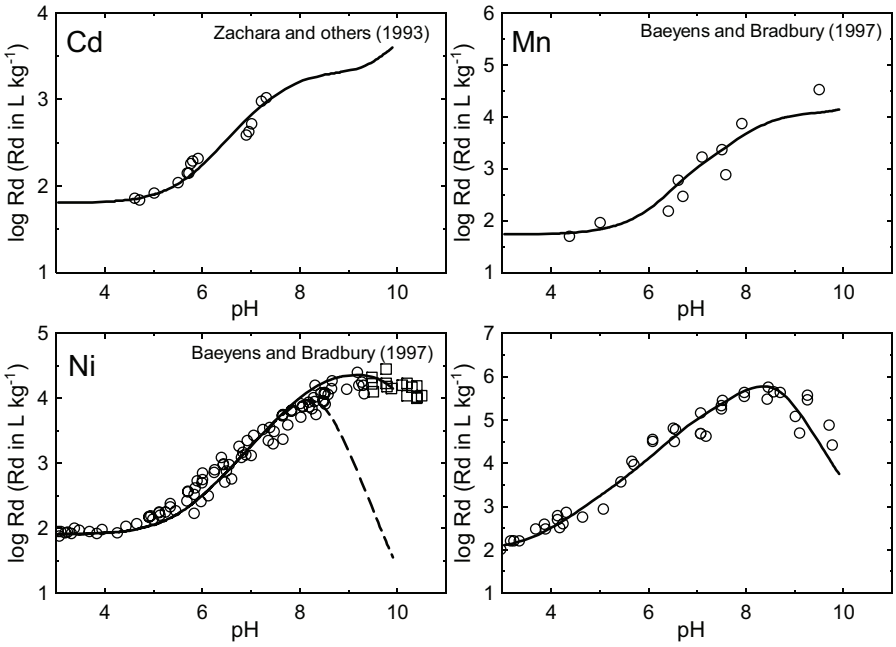

Fig. 13. Fit (lines) obtained with the "minimalist" approach for Zn, Mn, Ni, and Cd sorption data on strong sites (and cation exchange) of Swy-1 montmorillonite at I = 0.1 in $NaClO_4$ salt background (table 8). For Ni, the dashed line corresponds to the fit with maximum values for solute Ni hydrolysis constant while the solid line corresponds to minimum values. Squares correspond to data with probable (surface) precipitation.

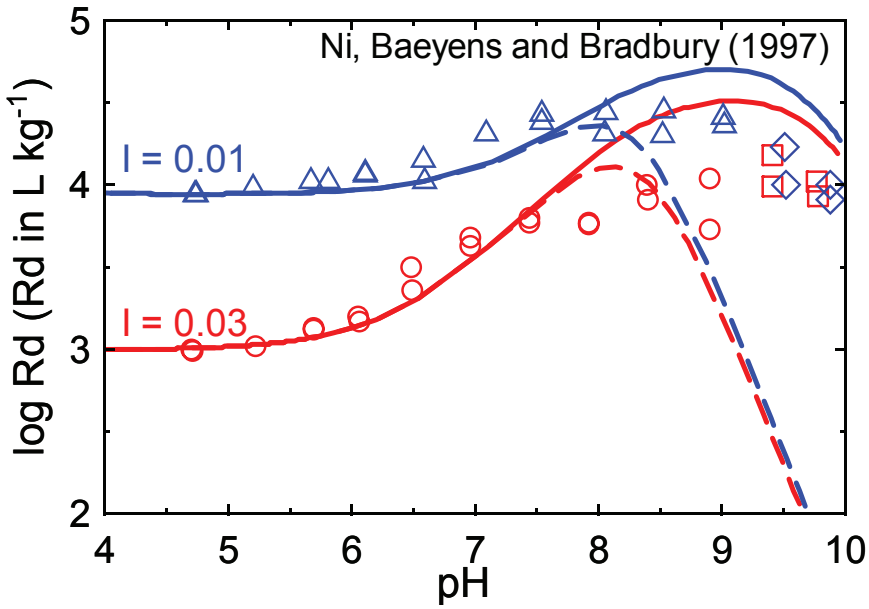

Fig. 14. Model prediction (lines) obtained with the "minimalist" approach for Ni sorption at low ionic strength in $NaClO_4$ on Swy-1. Squares and diamonds correspond to data with probable (surface) precipitation. The dashed line corresponds to the fit with maximum values for solute Ni hydrolysis constant while the solid line corresponds to minimum values.

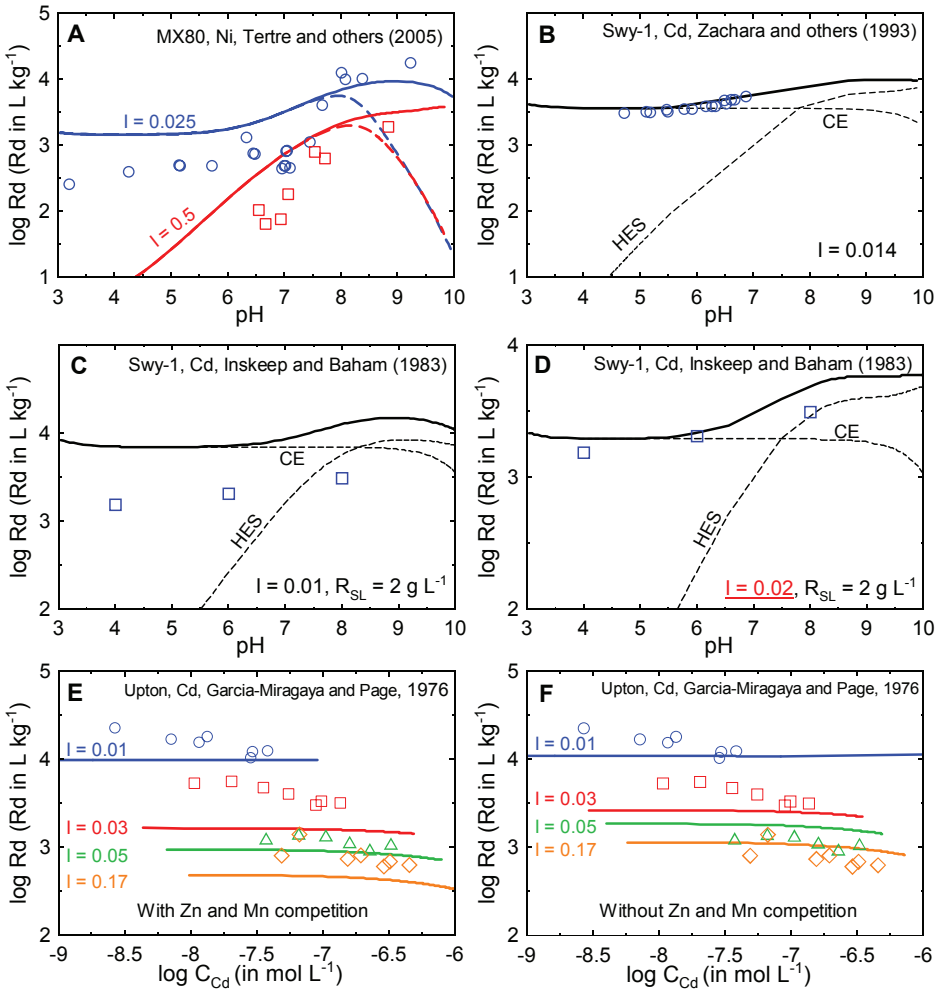

Fig. 15. Model prediction (solid lines) obtained with the "minimalist" approach for trace Cd and Ni sorption as a function of pH, ionic strength and Me concentration in $NaClO_4$ salt background (the nature of the solid, Me and data source are given in each figure). (A) the dashed line corresponds to the fit with maximum values for solute Ni hydrolysis constant while the solid line corresponds to minimum values. (B, C and D): the dashed and dotted lines correspond to the contribution of HES and cation exchange (CE) respectively. In (D), ionic strength was set at 0.02 for the model calculation (see text). (E) same Zn and Mn content in Upton montmorillonite as in Swy-1. (F) Zn and Mn concentrations were set at zero in the model (no competition).

strength of 0.01. This procedure should however end up with a solution having an ionic strength of 0.0192. With this value, a good agreement is obtained between modelled and measured Cd sorption values without changing the model parameters (fig. 15D). Results from Garcia-Miragaya and Page (1976) were also not well reproduced (fig. 15E), but these authors used a different clay material (Upton montmorillonite), with competing Zn and Mn contents that should in principle be different. Figure 15F shows that setting these competing cations at a concentration value of zero makes it possible to reproduce the data satisfactorily (an intermediate value making it possible to reproduce even better the experimental values; not shown). The remaining

discrepancy at lowest ionic strength (0.01 and 0.03) may be due to slightly different cation exchange selectivity coefficients of Upton and Swy-1 montmorillonites (see above for MX80 material). Also, slight changes in pH values with increasing Cd concentration could explain the observed discrepancies between model and data, as only an indicative pH range of 6.75 ± 0.25 is given by the authors.

Sorption prediction is also good for Ca salt background (fig. 16) when adding the effect of Ca competition for cation exchange sites (set here at a log K value of 0.8). No adjustment of the high energy site parameters is needed for Zn sorption. Ni sorption is slightly overestimated for high concentration of Ca. Cd sorption is also slightly overestimated by the model. In their revised model for Ca-montmorillonite, Bradbury and Baeyens (1999, 2005b) considered a decrease of affinity of Zn, Ni and Cd for HES in the presence of Ca in order to better fit the data but did not give any explanation for this change. In the Zn sorption curve (fig. 16B), two data points at pH ~ 10 are above the modeling curve for experiments in Ca salt background. Two affinity constants (for the formation of $\rangle SOZnOH$ and $\rangle SOZn(OH)_2^-$) were added in the 2SPNE SC/CE model in order to reproduce these two data points. These two parameters are thus very weakly constrained and it is not clear why these surface species would exist in Ca and not in Na salt backgrounds. This result could also be explained by side reactions: Zn co-precipitation with C-S-H-like phases could be promoted in the presence of Ca at high pH values with enhanced dissolution of clay or quartz. This type of artefact has already been observed by Tournassat and others (2004b) with an apparent increase in Ca sorption at high pH, which was due to C-S-H precipitation (Ferrage and others, 2005b). The same feature is also visible for the Cd sorption curve (fig. 16C). In this case, data in Na salt background are missing for comparison and the formation of the hydrolysed sorbed species might be justified.

Implications.—The non-electrostatic 2SPNE SC/CE modeling approach is very efficient and almost fulfils the requirements of the parsimony rule. Nonetheless, despite its simplicity, some of its parameters are not (or are very weakly) constrained by available data, namely the high energy site (de)protonation constants and the affinity constants for hydrolyzed $MeOH^+$ and $Me(OH)_2$ species. Although this has no influence on the prediction ability of the model for the metal (Zn, Ni, Cd) and clay (Swy-1) tested, it calls into question the validity of the LFER derived by Bradbury and Baeyens (2005b). This LFER is constrained only by modeled points that are not or are very weakly constrained by available data (log K_{HES} of $ZnOH^+$, $NiOH^+$, $MnOH^+$ *et cetera*, see table 8 and fig. 17). Although LFER relationships of this kind have been proven to be successful for oxides or hydroxides (Dzombak and Morel, 1990; Mathur and Dzombak, 2006), it is not the case for montmorillonite, according to our proposed minimalist approach.

Electrostatic Models: Some Reasons for Observed Failures

Although the minimalist approach is successful at describing Me sorption at HES (on Swy-1), it fails to take into account the electrostatic field effect on clay surfaces and therefore the physical reasons for its success remain unknown. A mechanistic surface complexation model must include an electrostatic term in order to agree with titration experiments.

In the general sorption equation (15), the electrostatic potential term, $-\left(\frac{(2-x)F\Psi_0}{RT\ ln\ 10}\right)$, depends on pH, and the surface potential Ψ_0 decreases with increasing pH (its absolute value increases). If the term relative to surface and solute speciation $log(K_{Me}R_{LS}[\rangle SOH_n]) - log\left(\frac{1}{\gamma_{div}} + \frac{K_{MeOH}}{\gamma_{mon}10^{-pH}} + \frac{K_{Me(OH)_2}K_{MeOH}}{10^{-2pH}}\right)$ is constant, then this change of Ψ_0 with pH results in a slope of log Rd *versus* pH higher than *x*. If

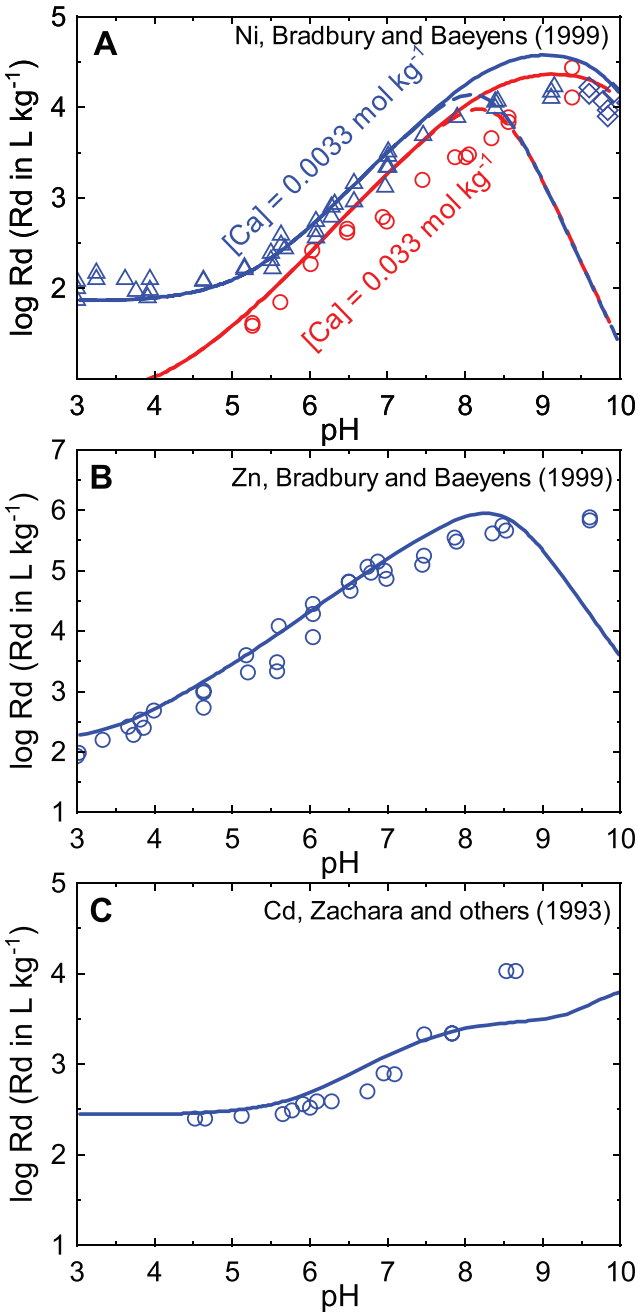

Fig. 16. Model prediction (lines) obtained with the "minimalist" approach for trace Zn, Cd and Ni sorption as a function of pH and ionic strength in $Ca(NO_3)_2$ or $Ca(ClO_4)_2$ salt background on Swy-1. (A) the dashed line corresponds to the fit with maximum values for solute Ni hydrolysis constant while the solid line corresponds to minimum values.

$x = 1$, the slope value is higher than one, in disagreement with sorption data (fig. 11). An agreement with the data can be found only by compensating the effect of the potential term by the effect of the surface speciation term.

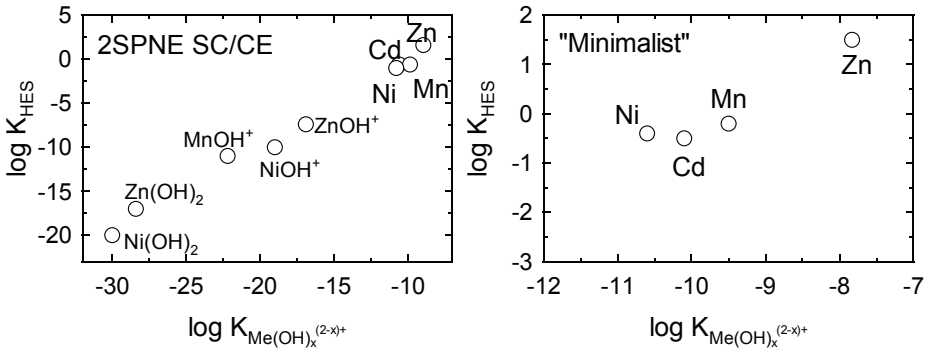

Fig. 17. Comparison of the LFER derived by Bradbury and Baeyens (2005b) for divalent metal cations with the LFER derived from our "minimalist" approach. Both approaches reproduce equally the same set of data.

In the following, the surface charge and potential model of Bourg and others (2007) will be considered. At I = 0.1, and for pH values between 4 and 8, its predicted edge surface potential can be approximated by a linear function:

$$\Psi_0 = a \times pH + b = -0.04058pH + 0.20009. \quad (17)$$

Combining equations (15) and (17):

$$log\ Rd = \left(x - \frac{(2-x)\mathrm{F} \times \mathrm{a}}{RT\ ln\ 10}\right)pH + log[\rangle \mathrm{SOH_n}] - log\left(\frac{1}{\gamma_{div}} + \frac{K_{MeOH}}{\gamma_{mon}10^{-pH}} + \frac{K_{Me(OH)_2}K_{MeOH}}{10^{-2pH}}\right) + log(K_{Me}R_{LS}) - \frac{(2-x)\mathrm{F} \times \mathrm{b}}{RT\ ln\ 10}. \quad (18)$$

If the speciation of HES remained constant over the pH range of interest, then the slope of log Rd *versus* pH would be $\left(x - \frac{(2-x)\mathrm{F} \times \mathrm{a}}{RT\ ln\ 10}\right) = 1.4$ for $x = 0$, 1.7 for $x = 1$ and 2 for $x = 2$, in disagreement with the experimentally determined slope of 1. Site hydrolysis is thus necessary:
with:

$$K_{Hyd} = \frac{[\rangle \mathrm{SOH^-_{n-1}}](\mathrm{H^+})}{[\rangle \mathrm{SOH_n}]}\ exp\left(-\frac{F\Psi_0}{RT}\right). \quad (19)$$

At trace metal concentration (low Me surface coverage) $[\rangle \mathrm{SOH_n}] + [\rangle \mathrm{SOH^-_{n-1}}] \approx [\rangle \mathrm{S_{tot}}]$ and thus:

$$log[\rangle \mathrm{SOH_n}] = log[\rangle \mathrm{S_{tot}}] - log\left(1 + \frac{K_{Hyd}}{10^{-pH}}\ exp\left(\frac{F(a \times pH + b)}{RT}\right)\right). \quad (20)$$

Combining equation (20) with equation (18):

$$log\ Rd = \left(x - \frac{(2-x)\mathrm{F} \times \mathrm{a}}{RT\ ln\ 10}\right)pH + log[\rangle \mathrm{S_{tot}}] - log\left(1 + \frac{K_{Hyd}}{10^{-pH}}\ exp\left(\frac{F(a \times pH + b)}{RT}\right)\right) - log\left(\frac{1}{\gamma_{div}} + \frac{K_{MeOH}}{\gamma_{mon}10^{-pH}} + \frac{K_{Me(OH)_2}K_{MeOH}}{10^{-2pH}}\right) + log(K_{Me}R_{LS}) - \frac{(2-x)\mathrm{F} \times \mathrm{b}}{RT\ ln\ 10}. \quad (21)$$

The linear part of the log Rd *versus* pH relationship with a slope of 1 implies that in this pH range:

$$log\ Rd \approx pH + A \tag{22}$$

where A is a constant. Considering that Me^{2+} is the main Me species in the same pH range, it implies in turn:

$$f(x, K_{Hyd}) = \left(x - \frac{(2-x)\mathrm{F} \times \mathrm{a}}{RT\ ln\ 10} - 1\right)pH - \frac{1}{ln\ 10}\ ln\left(1 + \frac{K_{Hyd}}{10^{-pH}}\ exp\left(\frac{F(a \times pH + b)}{RT}\right)\right)$$
$$= constant. \tag{23}$$

Therefore, an electrostatic model derived from the chosen surface charge and potential model can be applied to Me sorption on HES only if there is a couple of parameters K_{Hyd} and x that enables $f(x, K_{Hyd})$ to be constant in the pH range 4 to 8. This condition cannot be met for $x = 1$ or $x = 2$ (fig. 18). However, for $x = 0$, $f(x = 0, K_{Hyd})$ is almost constant for log K_{Hyd} values above -3. A value x equal to 0 corresponds to the reaction:

$$>SOH_n + Me^{2+} \rightleftharpoons SOH_nMe^{2+} \qquad \text{Reaction 9}$$

This result is in agreement with the results of Kraepiel and others (1999) who also noticed that this peculiar stoichiometry enabled them to fit Ni sorption data with their own electrostatic model. The large value of log K_{Hyd} means that most of the sorbing sites would be deprotonated ($\rangle SOH_{n-1}^-$) in the pH range 4 to 8.

We calculated Zn and Ni sorption (without competition) according to this surface speciation by solving numerically the full set of equations using equation (12) with $x = 0$ and using the surface speciation parameters available in Bourg and others (2007). Activity coefficients were computed using the Davies equation. K_{Hyd} and K_{Me} values were adjusted to match Zn and Ni sorption data at I = 0.1 in $NaClO_4$ background. A very acceptable fit can be found for $K_{Hyd} = -2$, $K_{Ni} = 7.4$ and $K_{Zn} = 9.3$ (fig. 19). However, data at I = 0.01 cannot be reproduced: the predicted Rd is far too high. Kraepiel and others (1999) noticed the same problem with their electrostatic sorption model. They also observed that this feature is completely masked when the data are plotted as a percentage of sorbed species as a function of pH, highlighting the need to work in log Rd representation for accurate modeling of sorption processes.

At high pH, the large increase in the modeled Rd value with decreasing ionic strength is due to an increased contribution of the potential term $\frac{(2-x)F\Psi_0}{RT\ ln\ 10}$ in equation (15). In oxide surface complexation models, the surface potential term changes very slightly from I = 0.1 to I = 0.01 for pH values between 6 and 10 where maximum cation sorption is observed. Moreover, the change in surface potential is weakly affected by the change in the surface charge, leading to an absence of ionic strength effect on predicted Me^{2+} sorption. Conversely, electrostatic models representative of montmorillonite surface result in large variations in the edge surface potential as a function of ionic strength due to the spill-over of basal potential. We calculated the increase in log Rd from I = 0.1 to I = 0.01 due to the variation in the potential term (for $x = 1$) according to the model of Bourg and others (2007). The calculation was performed for two K_{Hyd} values: 10^{-4} corresponding to a case where most of the sorption sites are in the form $\rangle SOH_{n-1}^-$, and 10^{-7} where most of the sorption sites are in the form $\rangle SOH_n$. At pH 8, where the sorption plateau is observed, the difference in log Rd (Δlog Rd) at I = 0.01 and I = 0.1 is 0.3 L kg^{-1} due to the surface potential change. This difference is small but corresponds to $x = 1$, a stoichiometry value that, in

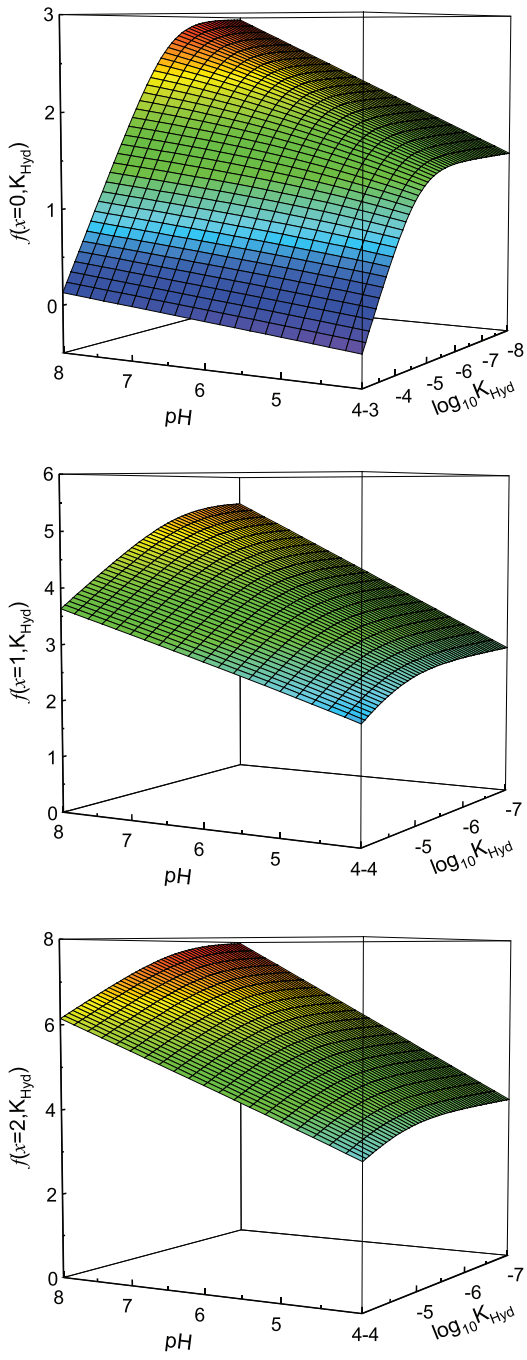

Fig. 18. Variation of $f(x, K_{Hyd})$ for $x = 0$ (top), $x = 1$ (middle) and $x = 2$ (bottom) as a function of pH and log K_{Hyd}.

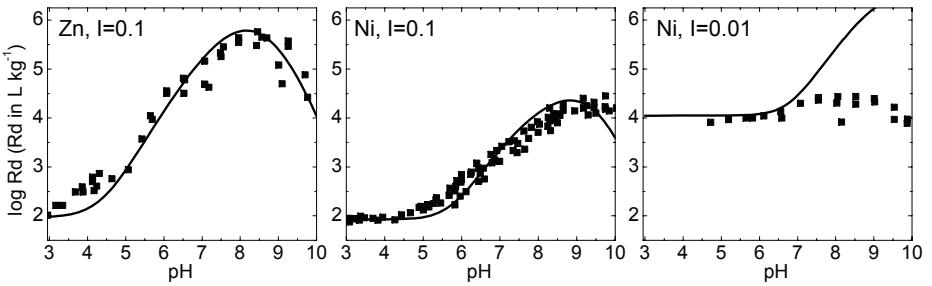

Fig. 19. Model prediction (lines) obtained with an electrostatic model using the mean field approach developed by Bourg and others (2007) together with Me sorption in the ⟩SOHMe^{2+} form. Zn and Ni sorption data in $NaClO_4$ background (symbols) are from Baeyens and Bradbury (1997). Left and middle figures: Zn and Ni sorption data at I = 0.1. Right figure: Ni sorption data at I = 0.01.

turn, is inappropriate to reproduce the log Rd *versus* pH slope value ($\leq$1). Using parameters that led to the best fit of the data ($x = 0$ and $\log K_{Hyd} > -4$, fig. 19), Δlog Rd cannot be less than 1 L kg^{-1} and increases with pH.

The above analysis demonstrates that any surface complexation model based on (i) the mean field theory for montmorillonite edge surface potential and (ii) the conventional description of the complexation reaction given by reaction 5 will fail to correctly describe HES sorption data as a function of pH (linear part of log Rd *versus* pH representation) and ionic strength (log Rd plateau at pH $\sim$ 8). The reasons for this failure lie either in the relevance of the mean field approximation for these sorption processes and/or in a lack in the identification of the true sorption mechanism and stoichiometry. The first point could be explored through molecular dynamics (MD) studies providing that their force field and surface representation could be proved adequate. This type of work is available for montmorillonite basal surfaces only and it is still limited to relatively high ionic strengths and high metal/clay ratios (Greathouse and Cygan, 2006; Tournassat and others, 2009; Bourg and Sposito, 2011). In the following, the second point is explored: shall our representation of HES sorption mechanism be changed?

An Attempt at Reconciling Montmorillonite Sorption Properties and Electrostatic Models

A substitution mechanism for sorption on HES.—The sorption reaction stoichiometry is an important feature of the model. There is no direct proof of the exact H^+/Me^{2+} stoichiometry for the sorption reaction on HES. Chemical species other than H^+ and Me^{2+} could also participate in the uptake reaction. It is worth noting the high number (from 2 to 5) of Si nearest-neighbors of Zn sorbed on HES sites (Dähn and others, 2011, and fig. 20). According to Churakov and others (2012), Zn is incorporated into the outermost trans-octahedra on (010) and (110) edges. A substitution of a structural atom from the edge surface by "sorbed" Zn is thus a preferred mechanism (another possible reaction is a concomitant sorption of Zn with Si in a kind of surface precipitation initiation).

In order to model this kind of reaction, we considered a Me-Mg substitution on the edge termination of the octahedral sheet. This Mg site is linked to an Al atom with a Mg-O-Al bridging oxygen and also has one or two OH groups in contact with water. Edge site valences appearing in equations (10)–(14) are obtained with Pauling's bond valence principle (Pauling, 1929). The protonation and deprotonation of this site can be modeled as follows:

$$>A1MgO_2H_3{}^{+1.33} \rightleftharpoons >A1MgO_2H_2{}^{+033} + H^+ \qquad K_{>MgO_2H_3} \qquad \text{Reaction 10}$$

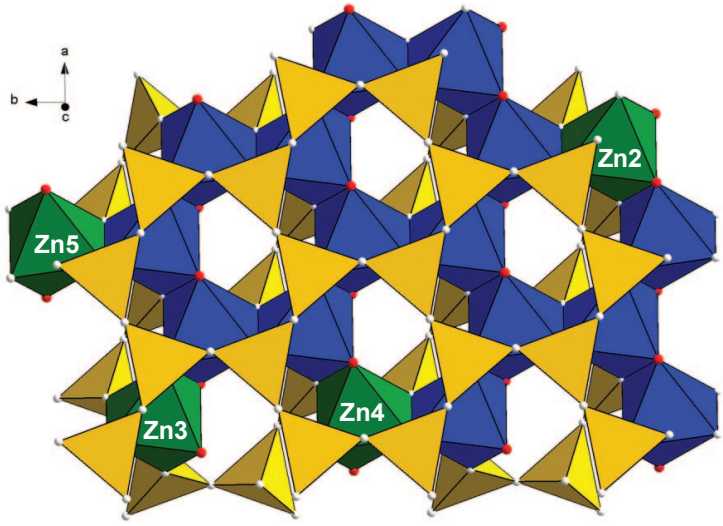

Fig. 20. Illustration of Zn sorbed on HES of montmorillonite edge surfaces, as probed by EXAFS analysis (after Dähn and others, 2011).

$$>A1MgO_2H_2^{+0.33} \rightleftharpoons >A1MgO_2H^{-0.67} + H^+ \qquad K_{>MgO_2H_2} \qquad \text{Reaction 11}$$

Mg^{2+} can be substituted by Me^{2+} as follows:

$$>A1MgO_2H_2^{+0.33} + Me^{2+} \rightleftharpoons >A1MeO_2H_2^{+0.33} + Mg^{2+} \qquad K_{>Mg\text{-}Me} \qquad \text{Reaction 12}$$

and this new surface site can deprotonate or protonate according to:

$$>A1MeO_2H_3^{+1.33} \rightleftharpoons >A1MeO_2H_2^{+0.33} + H^+ \qquad K_{>MeO_2H_3} \qquad \text{Reaction 13}$$

$$>A1MeO_2H_2^{+0.33} \rightleftharpoons >A1MeO_2H^{-0.67} + H^+ \qquad K_{>MeO_2H_2} \qquad \text{Reaction 14}$$

Reaction 12 is not affected by the electrostatic potential because charges of surface and solution remain identical before and after reaction: this type of reaction should make it possible to reproduce the sorption plateau region at pH ~ 8. Reaction 12 alone could not explain the pH dependency of Me sorption because H^+ is not part of the reaction equation. However, the difference in site protonation/deprotonation constants as a function of the nature of the cation attached to this site could drive the pH dependency of the sorption reaction.

We tested this substitution model using the electrostatic model of Bourg and others (2007) and a fitted amount of high energy reactive sites. Solute Mg concentration values were taken from Baeyens and Bradbury (1995). Mg concentration data were available for I = 0.5 only, and were assumed to be the same at I = 0.1 and I = 0.01. We approximated Mg concentration by two log-linear functions as a function of pH (fig. 21). Sorption calculations were performed with PHREEQC v2.18 (Parkhurst and Appelo, 1999), which does not include equation (11) for the calculation of edge surface potential as a function of pH and ionic strength. This problem was solved by defining a hypothetical additional surface charge σ_{add} in the PHREEQC input file in order to obtain $\Psi_{PHREEQC}(\sigma_0 + \sigma_{add}, pH, I) = \Psi_{Bourg}(\sigma_0, pH, I)$. $\Psi_{PHREEQC}$ is the surface potential calculated by PHREEQC with the DLM model and Ψ_{Bourg} is the surface potential of interest. The value of σ_{add} was adjusted for each pH and ionic strength condition. The accuracy of this calculation method is shown in figure 21 in

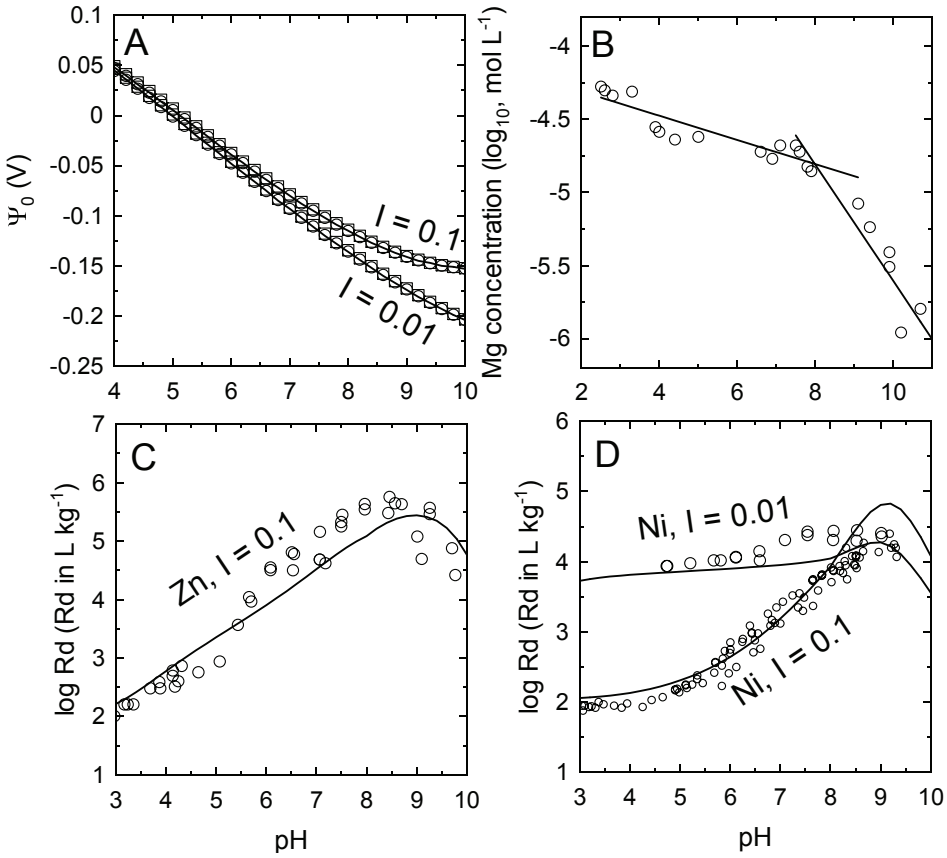

Fig. 21. (A) comparison of surface potentials determined as a function of pH and ionic strength with (i) the equation solver (Mathcad®) version of the Bourg and others (2007) model (solid lines), (ii) the PHREEQC version of the Bourg and others (2007) model (circles) and (ii) our "substitution" model (squares). (B) Mg concentration as a function of pH. Data (symbols) are from Baeyens and Bradbury (1995). (C and D) comparison of "substitution" model with Zn and Ni sorption data from Baeyens and Bradbury (1997).

the absence and in the presence of surface substitution sites. As a simplification of the model, we considered that (i) $K_{\rangle Mg\text{-}Me} = 1$ for Zn and Ni (no preference for site substitution), (ii) $K_{\rangle MgO_2H_3} = K_{\rangle MgO_2H_2}$ and (iii) $K_{\rangle MeO_2H_3} = K_{\rangle MeO_2H_2}$ for Me = Zn or Ni. Competition between Zn and Ni for sorption was considered in the calculation. This model fits the data fairly well with only four fitted parameters: $\log K_{\rangle MgO_2H_3} = -6.5$, $\log K_{\rangle ZnO_2H_3} = -2.2$, $\log K_{\rangle NiO_2H_3} = -3.6$ and the high energy site surface density (~2 mmol kg^{-1} for Swy-1 montmorillonite having an edge surface area of 19.2 $m^2\ g^{-1}$).

This substitution model is efficient. It is in agreement with an absence of ionic strength effect on the log Rd value at pH > 8 (the model predicts an even lower Rd at I = 0.01 than at I = 0.1 for pH > 8) and the 1:1 slope of log Rd *versus* pH is well reproduced without the need for a one H^+/one Me^{2+} stoichiometry. The competition effects between cations of similar charge can be taken into account. This model also predicts that there should be a competition effect of Mg for specific sorption sites. Hodgson (1960) showed that Mg was not able to displace significantly Co that was sorbed on HES of montmorillonite, but this observation is not in contradiction with our model prediction, because Mg concentration was 5×10^{-6} mol L^{-1}, that is in the

range of the concentration leached by the clay itself through desorption or dissolution. Our model predicts that a 10^{-3} mol L^{-1} Mg concentration should inhibit Zn and Ni sorption on HES. Available data in the presence of such a high Mg concentration are in agreement with an absence of high energy site contribution for Ni sorption (Montavon and others, 2006). However, these data were obtained on a montmorillonite with different sorption properties to Swy-1. Direct evidence of structural Mg release upon specific Me sorption does not exist for montmorillonite but is available for hectorite, a trioctahedral smectite. Addition of Zn to a hectorite suspension at pH 6.5 and at high ionic strength is followed by a release of Mg while Zn is sorbed (Schlegel and others, 2001a). This suggests a replacement of layer edge-exposed Mg by sorbed Zn. Experiments dedicated to understanding the exact reaction stoichiometry for Me sorption on montmorillonite HES are necessary to progress further in the modeling of their properties. For this task, solution composition should be analyzed beyond the conventional determination of pH, ionic strength and concentration of the metal of interest. We propose Mg as an additional element of interest. This additional element could be, however, Al^{3+} or another element present in trace amounts in the clay structure. The proposed model also has the advantage of explaining why reversibility is better achieved by decreasing pH (promoting dissolution, which is the reverse mechanism) than by decreasing Me concentration in solution (dilution methods impact the concentration of the competing structural cation as well). Finally, this surface substitution model is in line with findings concerning the epitaxial growth of Me-phyllosilicates upon sorption of larger Me concentrations (Schlegel and others, 1999a, 1999b; Schlegel and Manceau, 2006).

A state of the art electrostatic surface complexation model for LES.—It is necessary to have a sorption model for LES that is also coherent with the HES sorption model. The only mandatory common parameter between the two sorption models is the electrostatic potential because the sorption surface is the same for the two types of sites. Sorption on LES was implemented as a surface complexation reaction with aluminol sites, using the electrostatic model from Bourg and others (2007):

$$>AlOH^{-0.5} + Zn^{2+} \rightleftharpoons >AlOZn^{+0.5} + H^{+} \qquad K_{low\_Zn} \qquad \text{Reaction 15}$$

$$>AlOH^{-0.5} + Ni^{2+} \rightleftharpoons >AlONi^{+0.5} + H^{+} \qquad K_{low\_Ni} \qquad \text{Reaction 16}$$

Parameters of the complete model were adjusted to fit the data. They are given in table 9. The proposed electrostatic model describes the Zn and Ni sorption isotherm as well as the 2SPNE SC/CE model (fig. 22). Blind prediction exercises were also performed successfully on data from Ikhsan and others (2005) that probe low energy site reactivity (fig. 23). The proposed electrostatic sorption model is as efficient as the 2SPNE SC/CE or the minimalist non-electrostatic models.

CONCLUSIONS

Despite the numerous studies dedicated to montmorillonite sorption properties, no model from the literature is able to reproduce observed pH dependent specific sorption of divalent metals that also agrees with the electrostatic nature of montmorillonite surfaces. Modelers must avoid applying surface charge–surface potential relationships derived from oxide models directly to montmorillonite materials (and by extension to other clays): montmorillonite exhibits at least two types of surfaces with different electrostatic properties and whose properties are interconnected through the spill-over of basal electrostatic potential field on the edge surface potential. We have provided some guidance to build clay-specific surface complexation models with a set of reliable input parameters such as the edge reactive surface area. The latter must be determined by adequate methods (DIS, AFM) and not by the BET-method, which does not probe the surface of interest. Even in so doing, modeling divalent metal pH

TABLE 9

Parameters for the proposed electrostatic model (substitution for HES and surface complexation for LES). Cation exchange properties are taken identical to those given in the "minimalist" approach (table 8). All properties, with the exception of Me sorption properties, are taken from Bourg and others (2007).

Site type	Site density (sites nm^{-2})
>Si-OH	4.12
$>Al\text{-}OH^{-0.5}$	2.06-0.08
>AlAl-OH	2.06
$>SiAl\text{-}OH^{+0.5}$	2.06
$>AlMg\text{-}O_2H_2^{+0.33}$	0.08*

Reactions	Log K
$>Si\text{-}OH \rightleftharpoons >Si\text{-}O^- + H^+$	-11.1
$>Al\text{-}OH^{-0.5} + H^+ \rightleftharpoons >Al\text{-}OH_2^{+0.5}$	6.1
$>AlAl\text{-}OH + H^+ \rightleftharpoons >AlAl\text{-}OH_2^+$	5.1
$>AlMg\text{-}O_2H_2^{+0.33} + H^+ \rightleftharpoons >AlMg\text{-}O_2H_3^{+1.33}$	6.5
$>AlMg\text{-}O_2H_2^{+0.33} \rightleftharpoons >AlMg\text{-}O_2H^{-0.67} + H^+$	-6.5
$>AlMg\text{-}O_2H_2^{+0.33} + Zn^{2+} \rightleftharpoons >AlZn\text{-}O_2H_2^{+0.33} + Mg^{2+}$	0
$>AlMg\text{-}O_2H_2^{+0.33} + Ni^{2+} \rightleftharpoons >AlNi\text{-}O_2H_2^{+0.33} + Mg^{2+}$	0
$>AlZn\text{-}O_2H_2^{+0.33} + H^+ \rightleftharpoons >AlZn\text{-}O_2H_3^{+1.33}$	2.2
$>AlNi\text{-}O_2H_2^{+0.33} + H^+ \rightleftharpoons >AlNi\text{-}O_2H_3^{+1.33}$	3.8
$>AlZn\text{-}O_2H_2^{+0.33} \rightleftharpoons >AlZn\text{-}O_2H^{-0.67} + H^+$	2.2
$>AlNi\text{-}O_2H_2^{+0.33} \rightleftharpoons >AlNi\text{-}O_2H^{-0.67} + H^+$	3.8
$>Al\text{-}OH^{-0.5} + Zn^{2+} \rightleftharpoons >Al\text{-}OZn^{+0.5} + H^+$	-4
$>Al\text{-}OH^{-0.5} + Ni^{2+} \rightleftharpoons >Al\text{-}ONi^{+0.5} + H^+$	-5.7

* That is 2.5 mmol kg^{-1} for Swy-1 having an edge surface area of 19.2 $m^2\ g^{-1}$.

dependent specific sorption on clay edges is difficult. We have identified missing information, which is necessary to model sorption data in a mechanistic manner, together with experimental features that cast doubt on the ability of clay surface complexation models to describe adequately the nature of divalent metal sorption on montmorillonite edge surfaces. Problematic experimental features are mostly related to (i) the reversibility of sorption and (ii) the effect of the solid to liquid ratio on Rd measurements. Theoretically, surface complexation modeling is meaningful only in conditions where sorption is reversible and Rd measurements are independent of R_{SL}. Missing information includes (i) the exact reaction stoichiometries for sorption on HES and LES; (ii) reliable values for surface potential and charges as a function of

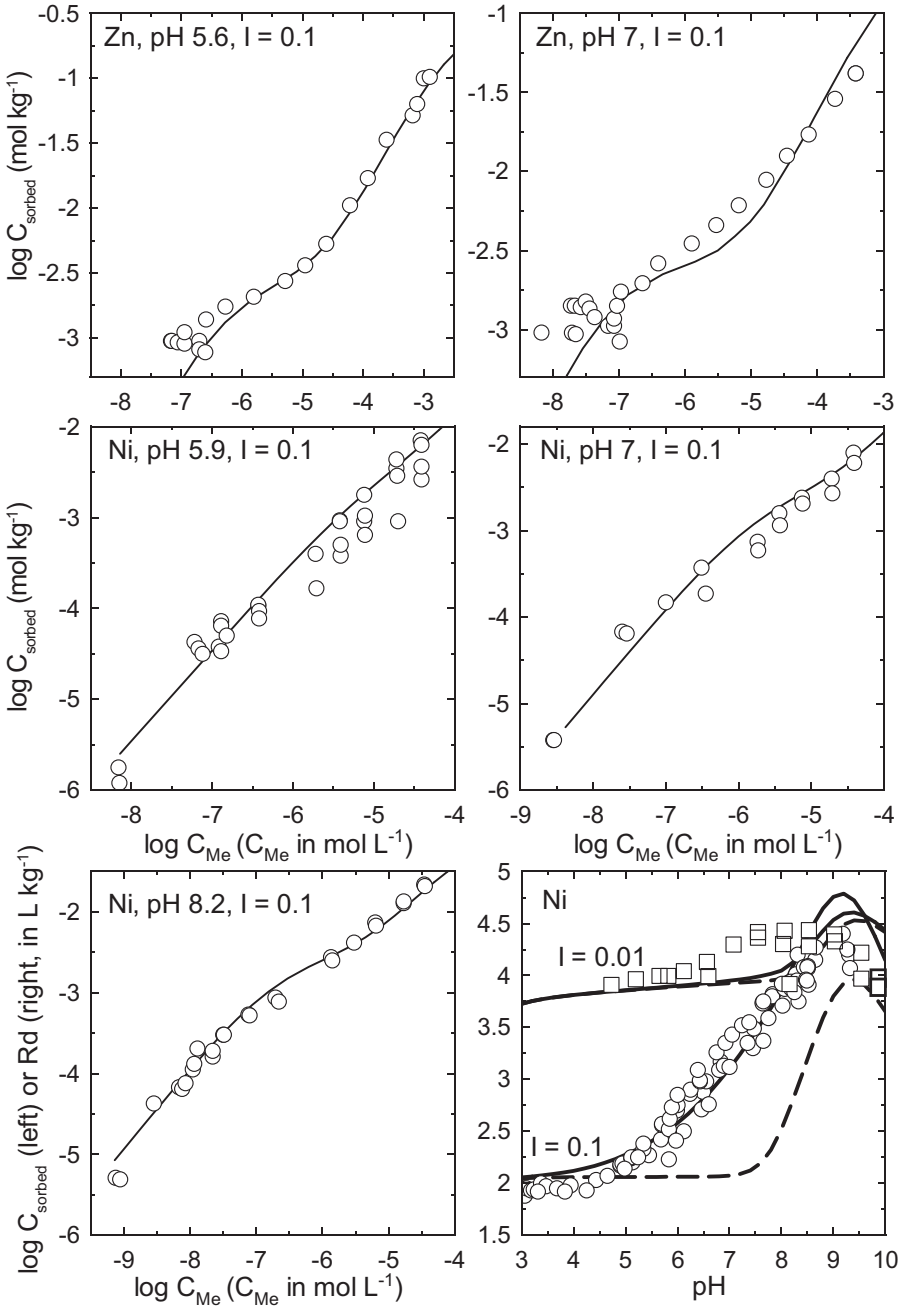

Fig. 22. Electrostatic model for HES (substitution model) and LES (surface complexation) according to the parameters given in table 9. Symbols: data from Baeyens and Bradbury (1997). Lines: model predictions. For Ni sorption edges, dashed lines indicate models without HES. The slope of log Zn sorbed *versus* log Zn ion solution is not well reproduced at pH 7 but this was also the case with the 2SPNE SC/CE model (see fig. 4 of the reference paper).

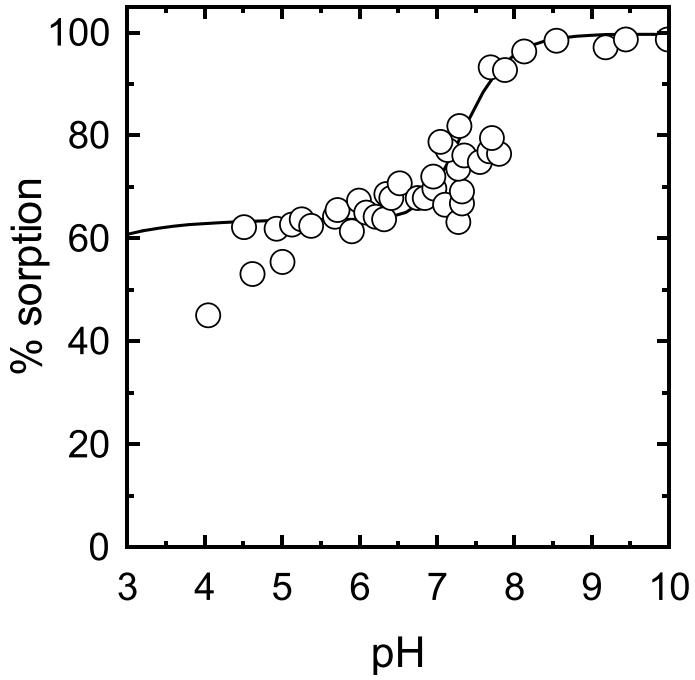

Fig. 23. Blind prediction of Zn sorption data from Ikhsan and others (2005) according to the parameters listed in table 9. An exchange selectivity coefficient for the Na-K reaction was fixed at a value of $\log K_{Na\text{-}K} = 0.8$ for modeling the low pH region (≤ 7).

ionic strength, pH and ionic background composition; and (iii) knowledge of the exact mechanism for sorption on HES.

Despite these limitations and assuming that selected data are representative of true thermodynamic surface/solution equilibriums, we could confirm that Me^{2+} pH dependent specific sorption mechanisms on HES and LES are different in nature. LES reactivity can be modeled with a state of the art electrostatic clay surface complexation model; HES cannot. HES sorption curve properties are not adequately reproduced by electrostatic surface complexation models because of two peculiar features: (i) a log Rd *versus* pH slope of one in the sorption edge region and (ii) a sorption plateau at pH 8 that is independent of ionic strength. These features are remarkably reproduced by non-electrostatic models, explaining the success of 2SPNE SC/CE models. An even simpler model than 2SPNE SC/CE models was proposed, following the rule of parsimony that eliminates unnecessary parameters. In so doing, we demonstrated that the reported LFER that links Me hydrolysis constants in solution to sorption constants is very weakly constrained for montmorillonite. Additional data are still needed to build an accurate LFER.

A change in the considered sorption reaction mechanism is necessary to model HES reactivity with the same electrostatic model as that used for LES. According to this approach, sorption on high energy sites would be the result of a structural substitution instead of a classically reported surface complexation mechanism. This result is in agreement with most recently reported spectroscopic and molecular modelling investigations. It enables measured sorption data to be reconciled with the electrostatic nature of clay surfaces. However, this substitution model still needs to be refined, especially regarding the nature(s) of the substituted cations in the clay layer.

ACKNOWLEDGMENTS

The results presented in this article were collected during the GL-Transfer Project granted by ANDRA in the framework of the ANDRA/BRGM scientific partnership. Professor W. H. Casey (Associat Editor), Professor B. Bickmore and two anonymous reviewers are warmly thanked for their constructive and helpful comments.

Appendix 1

CATION EXCHANGE MODELING

In the cation exchange theory, negatively charged sites are fully compensated by counter cations in the vicinity of the sites. In a sodium ionic medium, the reaction is expressed as:

$$2\,NaX + Me^{2+} \rightleftharpoons MeX_2 + 2\,Na^+ \qquad K_{ex}^{Na\rightarrow Me} \tag{A-1}$$

where X^- is a cation exchange site (due to the hypothesis given above, the concentration of free X^- sites is set at a value of 0, all of these sites being associated with Na^+ or other cations), Me^{2+} is a divalent metal cation and $K_{ex}^{Na\rightarrow Me}$ is the thermodynamic constant for the Na→Me exchange reaction:

$$K_{ex}^{Na\rightarrow Me} = \frac{(MeX_2)(Na^+)^2}{(NaX)^2(Me^{2+})} \tag{A-2}$$

where values in round brackets represent activities. Activity terms for the solute part of the equation are obtained using conventional computing methods for solute activity coefficients (for example Davies, Debye-Hückel, Pitzer). Conversely, the way to describe the activity of exchanged species is more problematic and there is no unifying theory to calculate the activity coefficients of exchanged species. They are usually defined as a fractional occupancy (*N* or *E*) of the exchanger times an activity coefficient. This fractional occupancy can be defined in two different conventions: a molar ratio convention (*N*, Vanselow convention) or an equivalent fraction convention (*E*, Gaines-Thomas convention). The question of the most appropriate convention has been widely debated in the literature and is not of primary interest for the present review. Most studies, including the present one, use the Gaines-Thomas convention with activity coefficient terms *g* set at 1 for all surface species in all conditions as an additional simplification (see Sposito, 1984 for details).

Appendix 2

EXAMPLE OF INCONSISTENT RESULTS REPORTED FOR METAL PRECIPITATION DURING A SORPTION EXPERIMENT

In order to avoid precipitation, which would lead to an overestimation of sorbed Ni, Baeyens and Bradbury (1995) conducted preliminary blank tests to determine the experimental pH/concentration range conditions in batch sorption tests for which no precipitation effects occurred. Following these tests, they decided to use a maximum $Ni(NO_3)_2$ concentration of 5×10^{-5} mol L^{-1} in isotherm experiments at

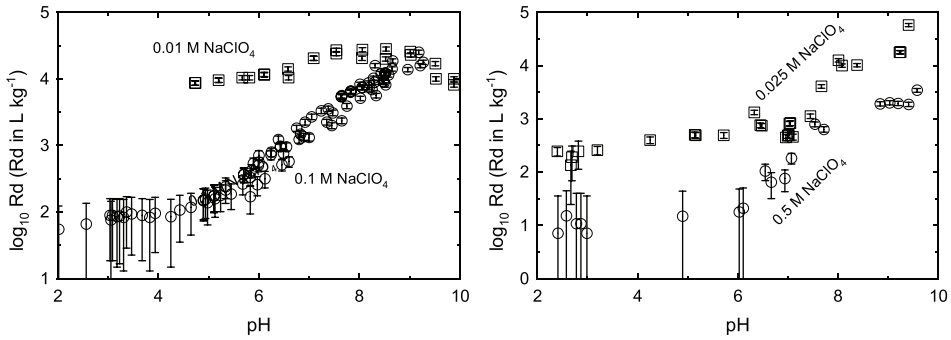

Fig. A1. Calculation of error bands with the experimental error propagation method. Application to data from Baeyens and Bradbury (1997, left figure) with $u(C_{eq}) = 2.5\% \times C_{eq}$ and $u(C_{init}) = 2.5\% \times C_{init}$; and Tertre and others (2005, right figure) with $u(C_{eq}) = 2.5\% \times C_{eq}$ for $C_{eq} > 5 \times 10^{-8}$ mol L^{-1} (10% otherwise) and $u(C_{init}) = 2.5\% \times C_{init}$.

pH 8.2, which is only slightly higher than the value determined from calculation. Contrastingly, Dähn and others (2002) did not detect any precipitation in a pH 8 solution containing 1.1×10^{-3} mol L^{-1} Ni over a time period of up to 1 year. Apparently, these two results are in disagreement (our understanding of the Baeyens and Bradbury experiment was initially that they obtained precipitation at concentrations greater than 5×10^{-5} mol L^{-1}). However, further examination of the tests carried out by these authors reveals that precipitation did not occur in their experiment below pH 8 for concentrations up to 10^{-4} mol L^{-1}, that is the maximum tested concentration). Losses in solute Ni activity were observed only for pH above pH 8 but were attributed to tube wall sorption. From these experimental clues, no precipitation occurs in the two previously cited references at Ni concentrations higher than those predicted by thermodynamic calculations. Two different hypotheses may be invoked to explain these contrasting results: (i) the solubility of crystalline $Ni(OH)_2$ is really higher than that recommended in Hummel and Curti (2003); and/or (ii) given the short equilibration time of Baeyens and Bradbury's (1997) experiments (2 days), precipitation of a crystalline $Ni(OH)_2$ product at 25 °C does not happen because of precipitation kinetics considerations. Data from Lothenbach and others (1997) tends to confirm this latter interpretation. Their Ni concentration is in remarkable agreement with calculated Ni solubility and their blank experiment showed a significant Ni concentration decrease after four weeks of equilibrium of an initial 10^{-4} mol L^{-1} Ni solution at pH 8, that is after a longer equilibration time than Baeyens and Bradbury's (1995) experiments. In turn, this result is also in contradiction with the above results presented by Dähn and others (2002). Because Lothenbach and others (1997) only acquired a single experimental data for Ni at pH 8, one could hypothesise that agreement with theory is fortuitous and that the observed aqueous Ni concentration decrease with time results from artefacts (for example, tube wall sorption). However, it is worth noting that the same agreement was also observed for Cd, Cu, Pb, and Zn. Thus, the probability that the observed aqueous Ni concentration decrease at pH 8 stems from an artefact is rather low. On the other hand, data from Dähn and others (2002) were acquired for a Ni concentration ten times higher than those of Lothenbach and others (1997). Thus, if Ni precipitation occurred in their preliminary experiments, the extent of Ni concentration decrease may have been within measurement uncertainty, a hypothesis reinforced by Ni^{2+} inertness at 25 °C (Hummel and Curti, 2003). From this analysis, it appears that these conflicting results cannot be solved.

Appendix 3

data uncertainties and pitfalls in data representation

Error calculation is crucial for data comparison. The present section focuses on the way errors are represented in the literature and compares them to a calculation method based on error propagation. The error on the percentage of sorbed metal, based on error propagation leads to:

$$u(\%\,sorption) = 100 \times \sqrt{\left(\frac{1}{C_{init}}\right)^2 u(C_{eq})^2 + \left(\frac{C_{eq}}{C_{init}^2}\right)^2 u(C_{init})^2} \tag{A-3}$$

provided that no covariance term applies, that is C_{eq} and C_{init} are measured independently. The uncertainty U (95.5% confidence, assuming normally distributed values, Danzer, 2007) is given by:

$$U(\%\,sorption) = 2 \times u(\%\,sorption). \tag{A-4}$$

For trace metal sorption and especially radionuclide sorption studies, results can be presented in log(Rd) *versus* pH or equilibrium concentration. Error propagation (neglecting uncertainty on solid/liquid ratio) leads to

$$u(Rd) = \sqrt{\left(\frac{L}{S}\frac{1}{C_{eq}}\right)^2 u(C_{init})^2 + \left(\frac{L}{S}\frac{C_{init}}{C_{eq}^2}\right)^2 u(C_{eq})^2}. \tag{A-5}$$

This representation offers several advantages, including a direct evaluation of the linear or non-linear characteristics of the sorption process. An additional advantage of this representation is the possibility of accurately representing sorption data at high (extreme) sorption levels. While percentage sorption representation would not make it possible to accurately visualize the difference between, for example, 99 and 99.9% sorption, Rd representation does. Note that measuring such a difference is very significant and relative uncertainties on measured Rd values are very low in these conditions (since $C_{eq} \ll C_{init}$):

$$\frac{u(Rd)}{Rd} \approx \sqrt{\left(\frac{u(C_{init})}{C_{init}}\right)^2 + \left(\frac{u(C_{eq})}{C_{eq}}\right)^2}. \tag{A-6}$$

Conversely, at low sorption levels, where the measurement error is at a maximum, Rd representation shrinks the information within a narrow range of values. Moreover, this representation prevents any accurate analysis of the data when actual associated uncertainties are not clearly indicated.

Rd results are frequently given in log representation. Uncertainties are given by:

$$U+ = \log(Rd + 2u(Rd)) - \log(Rd) \tag{A-7}$$

and

$$U- = \log(Rd) - \log(Rd - 2u(Rd)). \tag{A-8}$$

In that case, error bands are asymmetric and their extents (in log scale) decrease with increasing Rd. Surprisingly, most authors give symmetric error bands with constant extent, whatever the Rd values. If error bands are calculated with the error propagation method, it may be observed that the reproducibility of the measurement often fails to lie within the calculated error band extent, thus pointing to greater result variability than accounted for in the propagation error calculation. In short, the natural variability of the system exceeds the measurement repeatability (fig. A1).

These problems of data representation and error band calculation are repetitively addressed in the literature, especially in soil science (for example, Degryse and others, 2009) but, unfortunately, they are not taken enough into account in the sorption literature.

References

ANDRA, 2005, Référentiel du comportement des radionucléides et des toxiques chimiques d'un stockage dans le Callovo-Oxfordien jusqu'à l'Homme-Châtenay-Malabry, France, Dossier 2005 Argile, Agence Nationale pour la gestion des déchets radioactifs, Rapport Andra n°C.R.P.ASTR.04.0032

Avena, M. J., Mariscal, M. M., and De Pauli, C. P., 2003, Proton binding at clay surfaces in water: Applied Clay Science, v. 24, n. 1–2, p. 3–9, http://dx.doi.org/10.1016/j.clay.2003.07.003

Baeyens, B., and Bradbury, M. H., 1995, A quantitative mechanistic description of Ni, Zn and Ca sorption on Na-montmorillonite. Part I: Physico-chemical characterisation and titration measurements: Villigen, Paul Scherrer Institut (PSI), nr. 95-10 and Nagra NTB 95-04, p. 64.

——— 1997, A mechanistic description of Ni and Zn sorption on Na-montmorillonite. Part I: Titration and sorption measurements: Journal of Contaminant Hydrology, v. 27, n. 34, p. 199–222, http://dx.doi.org/10.1016/S0169-7722(97)00008-9

Barbier, F., Duc, G., and Petit-Ramel, M., 2000, Adsorption of lead and cadmium ions from aqueous solution to the montmorillonite/water interface: Colloids and Surfaces A—Physicochemical and Engineering Aspects, v. 166, n. 1, p. 153–159, http://dx.doi.org/10.1016/S0927-7757(99)00501-4

Bellenger, J. P., and Staunton, S., 2008, Adsorption and desorption of ^{85}Sr and ^{137}Cs on reference minerals, with and without inorganic and organic surface coatings: Journal of Environmental Radioactivity, v. 99, n. 5, p. 831–840, http://dx.doi.org/10.1016/j.jenvrad.2007.10.010

Bickmore, B. R., Hochella, M. F., Bosbach, D., and Charlet, L., 1999, Methods for performing atomic force microscopy imaging of clay minerals in aqueous solution: Clays and Clay Minerals, v. 47, n. 5, p. 573–581, http://dx.doi.org/10.1346/CCMN.1999.0470504

Bickmore, B. R., Rosso, K. M., Nagy, K. L., Cygan, R. T., and Tadanier, C. J., 2003, *Ab initio* determination of edge surface structures for dioctahedral 2:1 phyllosilicates: Implications for acid-base reactivity: Clays and Clay Minerals, v. 51, n. 4, p. 359–371, http://dx.doi.org/10.1346/CCMN.2003.0510401

Blanc, Ph., Lassin, A., Piantone, P., Azaroual, M., Jacquemet, N., Fabbri, A., and Gaucher, E. C., 2012, Thermoddem: A geochemical database focused on low temperature water/rock interactions and waste materials: Applied Geochemistry, v. 27, n. 10, p. 2107–2116, http://dx.doi.org/10.1016/j.apgeochem.2012.06.002

Bogolepov, A. A., 2009, Simulation of U(VI) and Co(II) sorption on montmorillonite: Radiochemistry (Moscow, Russian Federation) (Translation of Radiokhimiya), v. 51, n. 1, p. 96–103, http://dx.doi.org/10.1134/S1066362209010214

Bourg, I. C., and Sposito, G., 2011, Molecular dynamics simulations of the electrical double layer on smectite surfaces contacting concentrated mixed electrolyte ($NaCl$-$CaCl_2$) solutions: Journal of Colloid and Interface Science, v. 360, n. 2, p. 701–715, http://dx.doi.org/10.1016/j.jcis.2011.04.063

Bourg, I. C., Sposito, G., and Bourg, A. C. M., 2007, Modeling the acid-base surface chemistry of montmorillonite: Journal of Colloid and Interface Science, v. 312, n. 2, p. 297–310, http://dx.doi.org/10.1016/j.jcis.2007.03.062

Bradbury, M. H., and Baeyens, B., 1997a, Discussion on: "A mechanistic description of Ni and Zn sorption on Na-montmorillonite. Part I: Titration and sorption measurements. Part II: Modelling" by Bart Baeyens and Michael H. Bradbury—Reply to some comments: Journal of Contaminant Hydrology, v. 28, n. 1–2, p. 11–16, http://dx.doi.org/10.1016/S0169-7722(97)00002-8

——— 1997b, A mechanistic description of Ni and Zn sorption on Na-montmorillonite. Part II: modeling: Journal of Contaminant Hydrology, v. 27, p. 223–248, http://dx.doi.org/10.1016/S0169-7722(97)00007-7

——— 1999, Modeling the sorption of Zn and Ni on Ca-montmorillonite: Geochimica et Cosmochimica Acta, v. 63, n. 3–4, p. 325–336, http://dx.doi.org/10.1016/S0016-7037(98)00281-6
——— 2005a, Experimental measurements and modeling of sorption competition on montmorillonite: Geochimica et Cosmochimica Acta, v. 69, n. 17, p. 4187–4197, http://dx.doi.org/10.1016/j.gca.2005.04.014
——— 2005b, Modelling the sorption of Mn(II), Co(II), Ni(II), Zn(II), Cd(II), Eu(III), Am(III), Sn(IV), Th(IV), Np(V) and U(VI) on montmorillonite: Linear free energy relationships and estimates of surface binding constants for some selected heavy metals and actinides: Geochimica et Cosmochimica Acta, v. 69, n. 4, p. 875–892, http://dx.doi.org/10.1016/j.gca.2004.07.020
——— 2011, Predictive sorption modelling of Ni(II), Co(II), Eu(IIII), Th(IV) and U(VI) on MX-80 bentonite and Opalinus Clay: A "bottom-up" approach: Applied Clay Science, v. 52, n. 1–2, p. 27–33, http://dx.doi.org/10.1016/j.clay.2011.01.022
Brown, A. L., 1950, Zinc relationships in Aiken clay loam: Soil Science, v. 69, n. 5, p. 349–358, http://dx.doi.org/10.1097/00010694-195005000-00001
Chang, F. R. C., and Sposito, G., 1994, The electrical double layer of a disked-shaped clay mineral particle: effect of particle size: Journal of Colloid and Interface Science, v. 163, n. 1, p. 19–27, http://dx.doi.org/10.1006/jcis.1994.1076
——— 1996, The electrical double layer of a disked-shaped clay mineral particle: effects of electrolyte properties and surface charge density: Journal of Colloid and Interface Science, v. 178, n. 2, p. 555–564, http://dx.doi.org/10.1006/jcis.1996.0151
Charlet, L., Schindler, P. W., Spadini, L., Furrer, G., and Zysset, M., 1993, Cation adsorption on oxides and clays: The aluminum case: Aquatic Science, v. 55, n. 4, p. 291–303, http://dx.doi.org/10.1007/BF00877274
Churakov, S. V., 2006, *Ab initio* study of sorption on pyrophyllite: Structure and acidity of the edge sites: The Journal of Physical Chemistry B, v. 110, n. 9, p. 4135–4146, http://dx.doi.org/10.1021/jp053874m
Churakov, S. V., and Dähn, R., 2012, Zinc adsorption on clays inferred from atomistic simulations and EXAFS spectroscopy: Environmental Science & Technology, v. 46, n. 11, p. 5713–5719, http://dx.doi.org/10.1021/es204423k
Dähn, R., Scheidegger, A. M., Manceau, A., Schlegel, M. L., Baeyens, B., Bradbury, M. H., and Morales, M., 2002, Neoformation of Ni phyllosilicate upon Ni uptake on montmorillonite: A kinetics study by powder and polarized extended X-ray absorption fine structure spectroscopy: Geochimica et Cosmochimica Acta, v. 66, n. 13, p. 2335–2347, http://dx.doi.org/10.1016/S0016-7037(02)00842-6
Dähn, R., Scheidegger, A. M., Manceau, A., Schlegel, M., Baeyens, B., Bradbury, M. H., and Chateigner, D. L., 2003, Structural evidence for the sorption of Ni(II) atoms on the edges of montmorillonite clay minerals: A polarized X-ray absorption fine structure study: Geochimica et Cosmochimica Acta, v. 67, p. 1–15, http://dx.doi.org/10.1016/S0016-7037(02)01005-0
Dähn, R., Baeyens, B., and Bradbury, M. H., 2011, Investigation of the different binding edge sites for Zn on montmorillonite using P-EXAFS—The strong/weak site concept in the 2SPNE SC/CE sorption model: Geochimica et Cosmochimica Acta, v. 75, n. 18, p. 5154–5168, http://dx.doi.org/10.1016/j.gca.2011.06.025
Danzer, K., 2007, Analytical chemistry, Theoretical and metrological fundamentals: Heidelberg, Springer, 315 p.
De Mumbrum, L. E., and Jackson, M. L., 1956, Infrared absorption evidence on exchange reaction mechanism of copper and zinc with layer silicate clays and peat: Soil Science Society of America Journal, v. 20, n. 3, p. 334–337, http://dx.doi.org/10.2136/sssaj1956.03615995002000030010x
Degryse, F., Smolders, E., and Parker, D. R., 2009, Partitioning of metals (Cd, Co, Cu, Ni, Pb, Zn) in soils: concepts, methodologies, prediction and applications—a review: European Journal of Soil Science, v. 60, n. 4, p. 590–612, http://dx.doi.org/10.1111/j.1365-2389.2009.01142.x
Delhorme, M., Labbez, C., Caillet, C., and Thomas, F., 2010, Acid-base properties of 2:1 clays. I. Modeling the role of electrostatics: Langmuir, v. 26, n. 12, p. 9240–9249, http://dx.doi.org/10.1021/la100069g
Di Toro, D. M., Mahony, J. D., Kirchgraber, P. R., Obyrne, A. L., Pasquale, L. R., and Piccirilli, D. C., 1986, Effects of nonreversibility, particle concentration, and ionic-strength on heavy-metal sorption: Environmental Science & Technology, v. 20, n. 1, p. 55–61, http://dx.doi.org/10.1021/es00143a006
Donat, R., Akdogan, A., Erdem, E., and Cetish, H., 2005, Thermodynamics of Pb^{2+} and Ni^{2+} adsorption onto natural bentonite from aqueous solutions: Journal of Colloid and Interface Science, v. 286, n. 1, p. 43–52, http://dx.doi.org/10.1016/j.jcis.2005.01.045
Duc, M., Gaboriaud, F., and Thomas, F., 2005a, Sensitivity of the acid-base properties of clays to the methods of preparation and measurement: 1. Literature review: Journal of Colloid and Interface Science, v. 289, n. 1, p. 139–147, http://dx.doi.org/10.1016/j.jcis.2005.03.060
——— 2005b, Sensitivity of the acid-base properties of clays to the methods of preparation and measurement: 2. Evidence from continuous potentiometric titrations: Journal of Colloid and Interface Science, v. 289, n. 1, p. 148–156, http://dx.doi.org/10.1016/j.jcis.2005.03.057
Dzombak, D. A., and Morel, F. M. M., 1990, Surface complexation modeling—Hydrous ferric oxide: New York, Wiley-Interscience, 393 p.
Egozy, Y., 1980, Adsorption of cadmium and cobalt on montmorillonite as a function of solution composition: Clays and Clay Minerals, v. 28, n. 4, p. 311–318, http://dx.doi.org/10.1346/CCMN.1980.0280410
Farrah, H., Hatton, D., and Pickering, W. F., 1980, The affinity of metal-ions for clay surfaces: Chemical Geology, v. 28, p. 55–68, http://dx.doi.org/10.1016/0009-2541(80)90035-2
Ferrage, E., Lanson, B., Sakharov, B. A., and Drits, V. A., 2005a, Investigation of smectite hydration properties by modeling experimental X-ray diffraction patterns: Part I. Montmorillonite hydration properties: American Mineralogist, v. 90, n. 8–9, p. 1358–1374, http://dx.doi.org/10.2138/am.2005.1776

Ferrage, E., Tournassat, C., Rinnert, E., and Lanson, B., 2005b, Influence of pH on the interlayer cationic composition and hydration state of Ca-montmorillonite: Analytical chemistry, chemical modelling and XRD profile modelling study: Geochimica et Cosmochimica Acta, v. 69, n. 11, p. 2797–2812, http://dx.doi.org/10.1016/j.gca.2004.12.008

Fomina, M., and Gadd, G. M., 2002, Influence of clay minerals on the morphology of fungal pellets: Mycological Research, v. 106, n. 1, p. 107–117, http://dx.doi.org/10.1017/S0953756201004786

Garcia-Miragaya, J., and Page, A. L., 1976, Influence of ionic-strength and inorganic complex-formation on sorption of trace amounts of Cd by montmorillonite: Soil Science Society of America Journal, v. 40, n. 5, p. 658–633, http://dx.doi.org/10.2136/sssaj1976.03615995004000050019x

Garcia-Miragaya, J., Cardenas, R., and Page, A. L., 1986, Surface loading effect on Cd and Zn sorption by kaolinite and montmorillonite from low concentration solutions: Water Air and Soil Pollution, v. 27, n. 1–2, p. 181–190, http://dx.doi.org/10.1007/BF00464780

Ghayaza, M., Le Forestier, L., Muller, F., Tournassat, C., and Beny, J. M., 2011, Pb(II) and Zn(II) adsorption onto Na- and Ca-montmorillonites in acetic acid/acetate medium: Experimental approach and geochemical modeling: Journal of Colloid and Interface Science, v. 361, n. 1, p. 238–246, http://dx.doi.org/10.1016/j.jcis.2011.05.028

Glaus, M. A., Baeyens, B., Lauber, M., Rabung, T., and Van Loon, L. R., 2005, Influence of water-extractable organic matter from Opalinus Clay on the sorption and speciation of Ni(II), Eu(III) and Th(IV): Applied Geochemistry, v. 20, n. 2, p. 443–451, http://dx.doi.org/10.1016/j.apgeochem.2004.09.004

Grambow, B., Fattahi, M., Montavon, G., Moisan, C., and Giffaut, E., 2006, Sorption of Cs, Ni, Pb, Eu(III), Am(III), Cm, Ac(III), Tc(IV), Th, Zr, and U(VI) on MX80 bentonite: An experimental approach to assess model uncertainty: Radiochimica Acta, v. 94, p. 627–636, http://dx.doi.org/10.1524/ract.2006.94.9-11.627

Greathouse, J. A., and Cygan, R. T., 2006, Water structure and aqueous uranyl(VI) adsorption equilibria onto external surfaces of beidellite, montmorillonite, and pyrophyllite: Results from molecular simulations: Environmental Science & Technology, v. 40, n. 12, p. 3865–3871, http://dx.doi.org/10.1021/es052522q

Green-Pedersen, H., and Pind, N., 2000, Preparation, characterization, and sorption properties for Ni(II) of iron oxyhydroxide-montmorillonite: Colloids and Surfaces A—Physicochemical and Engineering Aspects, v. 168, n. 2, p. 133–145, http://dx.doi.org/10.1016/S0927-7757(00)00448-9

Green-Pedersen, H., Jensen, B. T., and Pind, N., 1997, Nickel adsorption on MnO_2, $Fe(OH)_{(3)}$, montmorillonite, humic acid and calcite: A comparative study: Environmental Technology, v. 18, n. 8, p. 807–815, http://dx.doi.org/10.1080/09593331808616599

Gu, X. Y., Evans, L. J., and Barabash, S. J., 2010, Modeling the adsorption of Cd (II), Cu (II), Ni (II), Pb (II) and Zn (II) onto montmorillonite: Geochimica et Cosmochimica Acta, v. 74, n. 20, p. 5718–5728, http://dx.doi.org/10.1016/j.gca.2010.07.016

Hibbard, P. O., 1940, The chemical status of zinc in the soil with methods of analysis: Hilgardia, v. 13, p. 1–29.

Hiemstra, T., and Van Riemsdijk, W. H., 1996, A surface structural approach to ion adsorption: The charge distribution (CD) model: Journal of Colloid and Interface Science, v. 179, n. 2, p. 488–508, http://dx.doi.org/10.1006/jcis.1996.0242

Hiemstra, T., Van Riemsdijk, W. H., and Bolt, G. H., 1989, Multisite proton adsorption modelling at the solid/solution interface of (hydr)oxides: A new approach. I. Model description and evaluation of intrinsic reaction constants: Journal of Colloid and Interface Science, v. 133, n. 1, p. 91–104, http://dx.doi.org/10.1016/0021-9797(89)90284-1

Hodgson, J. F., 1960, Cobalt reactions with montmorillonite: Soil Science Society of America Proceedings, v. 24, n. 3, p. 165–168, http://dx.doi.org/10.2136/sssaj1960.03615995002400030013x

Hu, J., Xu, D., Chen, L., and Wang, X. K., 2009, Characterization of MX-80 bentonite and its sorption of radionickel in the presence of humic and fulvic acids: Journal of Radioanalytical and Nuclear Chemistry, v. 279, n. 3, p. 701–708, http://dx.doi.org/10.1007/s10967-007-7252-6

Hummel, W., and Curti, E., 2003, Nickel aqueous speciation and solubility at ambient conditions: A thermodynamic elegy: Monatshefte Fur Chemie, v. 134, n. 7, p. 941–973, http://dx.doi.org/10.1007/s00706-003-0010-8

Ikhsan, J., Wells, J. D., Johnson, B. B., and Angove, M. J., 2005, Surface complexation modeling of the sorption of Zn(II) by montmorillonite: Colloids and Surfaces A: Physicochemical and Engineering Aspects, v. 252, n. 1, p. 33–41, http://dx.doi.org/10.1016/j.colsurfa.2004.10.011

Inskeep, W. P., and Baham, J., 1983, Adsorption of Cd(II) and Cu(II) by Na-montmorillonite at low surface coverage: Soil Science Society of America Journal, v. 47, n. 4, p. 660–665, http://dx.doi.org/10.2136/sssaj1983.03615995004700040011x

Jones, H. W., Gall, O. E., and Barnett, R. M., 1936, The reaction of zinc sulphate with the soil: Florida Agricultural Experimental Station Bulletin, v. 298, p. 5–43.

Kraepiel, A. M. L., Keller, K., and Morel, F. M. M., 1998, On the acid-base chemistry of permanently charged minerals: Environmental Science & Technology, v. 32, n. 19, p. 2829–2838, http://dx.doi.org/10.1021/es9802899

——— 1999, A model for metal adsorption on montmorillonite: Journal of Colloid and Interface Science, v. 210, n. 1, p. 43–54, http://dx.doi.org/10.1006/jcis.1998.5947

Kul, A. R., and Koyuncu, H., 2010, Adsorption of Pb(II) ions from aqueous solution by native and activated bentonite: Kinetic, equilibrium and thermodynamic study: Journal of Hazardous Materials, v. 179, n. 1–3, p. 332–339, http://dx.doi.org/10.1016/j.jhazmat.2010.03.009

Kulik, D. A., 2002a, Gibbs energy minimization approach to modeling sorption equilibria at the mineral-water interface: Thermodynamic relations for multi-site-surface complexation: American Journal of Science, v. 302, n. 3, p. 227–279, http://dx.doi.org/10.2475/ajs.302.3.227

——— 2002b, Sorption modelling by Gibbs energy minimisation: Towards a uniform thermodynamic database for surface complexes of radionuclides: Radiochimica Acta, v. 90, p. 815–832, http://dx.doi.org/10.1524/ract.2002.90.9-11_2002.815
——— 2009, Thermodynamic concepts in modeling sorption at the mineral-water interface, *in* Oelkers, E. H, and Schott, J., editors, Thermodynamics and Kinetics of Water-Rock Interaction: Reviews in Mineralogy and Geochemistry, v. 70, p. 125–180, http://dx.doi.org/10.2138/rmg.2009.70.4
Le Forestier, L., Muller, F., Villieras, F., and Pelletier, M., 2010, Textural and hydration properties of a synthetic montmorillonite compared with a natural Na-exchanged clay analogue: Applied Clay Science, v. 48, n. 1–2, p. 18–25, http://dx.doi.org/10.1016/j.clay.2009.11.038
Lee, S., Anderson, P. R., Bunker, G. B., and Karanfil, C., 2004, EXAFS study of Zn sorption mechanisms on montmorillonite: Environmental Science & Technology, v. 38, n. 20, p. 5426–5432, http://dx.doi.org/10.1021/es0350076
Leroy, P., Tournassat, C., and Bizi, M., 2011, Influence of surface conductivity on the apparent zeta potential of TiO_2 nanoparticles: Journal of Colloid and Interface Science, v. 356, n. 2, p. 442–453, http://dx.doi.org/10.1016/j.jcis.2011.01.016
Limousin, G., Gaudet, J. P., Charlet, L., Szenknect, S., Barthes, V., and Krimissa, M., 2007, Sorption isotherms: A review on physical bases, modeling and measurement: Applied Geochemistry, v. 22, n. 2, p. 249–275, http://dx.doi.org/10.1016/j.apgeochem.2006.09.010
Lothenbach, B., Furrer, G., and Schulin, R., 1997, Immobilization of heavy metals by polynuclear aluminium and montmorillonite compounds: Environmental Science & Technology, v. 31, n. 5, p. 1452–1462, http://dx.doi.org/10.1021/es960697h
Lothenbach, B., Furrer, G., Scharli, H., and Schulin, R., 1999, Immobilization of zinc and cadmium by montmorillonite compounds: Effects of aging and subsequent acidification: Environmental Science & Technology, v. 33, n. 17, p. 2945–2952, http://dx.doi.org/10.1021/es981317q
Marcussen, H., Holm, P. E., Strobel, B. W., and Hansen, H. Chr. B., 2009, Nickel sorption to goethite and montmorillonite in presence of citrate: Environmental Science & Technology, v. 43, n. 4, p. 1122–1127, http://dx.doi.org/10.1021/es801970z
Mathur, S. S., and Dzombak, D. A., 2006, Surface complexation modeling: Goethite, *in* Lützenkirchen, J., editor, Surface Complexation Modelling, chapter 16: Amsterdam, Elsevier, Interface Science and Technology, v. 11, p. 443–468.
McBride, M. B., 1997, A critique of diffuse double layer models applied to colloid and surface chemistry: Clays and Clay Minerals, v. 45, n. 4, p. 598–608, http://dx.doi.org/10.1346/CCMN.1997.0450412
Miller, A. W., and Wang, Y. F., 2012, Radionuclide interaction with clays in dilute and heavily compacted systems: A critical review: Environmental Science & Technology, v. 46, n. 4, p. 1981–1994, http://dx.doi.org/10.1021/es203025q
Montavon, G., Alhajji, E., and Grambow, B., 2006, Study of the interaction of Ni^{2+} and Cs^{+} on MX-80 bentonite; Effect of compaction using the "capillary method": Environmental Science & Technology, v. 40, n. 15, p. 4672–4679, http://dx.doi.org/10.1021/es052483i
Morton, J. D., Semrau, J. D., and Hayes, K. F., 2001, An X-ray absorption spectroscopy study of the structure and reversibility of copper adsorbed to montmorillonite clay: Geochimica et Cosmochimica Acta, v. 65, n. 16, p. 2709–2722, http://dx.doi.org/10.1016/S0016-7037(01)00633-0
Papelis, C., and Hayes, K. F., 1996, Distinguishing between interlayer and external sorption sites of clay minerals using X-ray absorption spectroscopy: Colloids and Surfaces A: Physicochemical and Engineering Aspects, v. 107, p. 89–96, http://dx.doi.org/10.1016/0927-7757(95)03370-X
Parkhurst, D. L., and Appelo, C. A. J., 1999, User's guide to PHREEQC (Version 2)—A computer program for speciation, batch-reaction, one-dimensional transport, and inverse geochemical calculations, Water-resources investigations: U.S. Geological Survey Water Resources Investigations Report 99-4259, 312 p.
Pauling, L., 1929, The principles determining the structure of complex ionic crystals: Journal of American Chemical Society, v. 51, n. 4, p. 1010–1026, http://dx.doi.org/10.1021/ja01379a006
Peigneur, P., Maes, A., and Cremers, A., 1975, Heterogeneity of charge density distribution in montmorillonite as inferred from cobalt adsorption: Clays and Clay Minerals, v. 23, p. 71–75, http://dx.doi.org/10.1346/CCMN.1975.0230110
Perronnet, M., Villiéras, F., Jullien, M., Razafitianamaharavo, A., Raynal, J., and Bonnin, D., 2007, Towards a link between the energetic heterogeneities of the edge faces of smectites and their stability in the context of metallic corrosion: Geochimica et Cosmochimica Acta, v. 71, n. 6, p. 1463–1479, http://dx.doi.org/10.1016/j.gca.2006.12.011
Scheidegger, A. M., Lamble, G. M., and Sparks, D. L., 1997, Spectroscopic evidence for the formation of mixed-cation hydroxide phases upon metal sorption on clays and aluminum oxides: Journal of Colloid and Interface Science, v. 186, n. 1, p. 118–128, http://dx.doi.org/10.1006/jcis.1996.4624
Schindler, P. W., and Gamsjäger, H., 1972, Acid-base reactions of the TiO_2 (anatase)-water interface and the point of charge of TiO_2 suspensions: Kolloid Zeitschrift Pollymere (Colloid and Polymer Science), v. 250, n. 7, p. 759–763, http://dx.doi.org/10.1007/BF01498568
Schindler, P. W., and Stumm, W., 1987, The surface chemistry of oxides, hydroxides and oxide minerals, *in* Stumm, W., editor, Aquatic Surface Chemistry: New-York, Wiley Interscience, p. 311–338.
Schlegel, M. L., and Manceau, A., 2006, Evidence for the nucleation and epitaxial growth of Zn phyllosilicate on montmorillonite: Geochimica et Cosmochimica Acta, v. 70, n. 4, p. 901–917, http://dx.doi.org/10.1016/j.gca.2005.10.021
Schlegel, M. L., Charlet, L., and Manceau, A., 1999a, Sorption of metal ions on clay minerals: II. Mechanism of Co sorption on hectorite at high and low ionic strength and impact on the sorbent stability: Journal of Colloid and Interface Science, v. 220, n. 2, p. 392–405, http://dx.doi.org/10.1006/jcis.1999.6538
Schlegel, M. L., Manceau, A., Chateigner, D. L., and Charlet, L., 1999b, Sorption of metal ions on clay minerals: I. Polarized EXAFS evidence for the adsorption of Co on the edges of hectorite particles:

Journal of Colloid and Interface Science, v. 215, n. 1, p. 140–158, http://dx.doi.org/10.1006/jcis.1999.6253
Schlegel, M. L., Manceau, A., Charlet, L., and Hazemann, J. L., 2001a, Adsorption mechanisms of Zn on hectorite as a function of time, pH, and ionic strength: American Journal of Science, v. 301, n. 9, p. 798–830, http://dx.doi.org/10.2475/ajs.301.9.798
Schlegel, M. L., Manceau, A., Charlet, L., Chateigner, D. L., and Hazemann, J. L., 2001b, Sorption of metal ions on clay minerals. III. Nucleation and epitaxial growth of Zn phyllosilicate on the edges of hectorite: Geochimica et Cosmochimica Acta, v. 65, n. 22, p. 4155–4170, http://dx.doi.org/10.1016/S0016-7037(01)00700-1
Schramm, L. L., and Kwak, J. C. T., 1982, Influence of exchangeable cation composition on the size and shape of montmorillonite particles in dilute suspension: Clays and Clay Minerals, v. 30, n. 1, p. 40–48, http://dx.doi.org/10.1346/CCMN.1982.0300105
Secor, R. B., and Radke, C. J., 1985, Spillover of the diffuse double-layer on montmorillonite particles: Journal of Colloid and Interface Science, v. 103, n. 1, p. 237–244, http://dx.doi.org/10.1016/0021-9797(85)90096-7
Sen Gupta, S., and Bhattacharyya, K. G., 2008, Immobilization of Pb(II), Cd(II) and Ni(II) ions on kaolinite and montmorillonite surfaces from aqueous medium: Journal of Environmental Management, v. 87, n. 1, p. 46–58, http://dx.doi.org/10.1016/j.jenvman.2007.01.048
Solomon, T., 2001, The definition and unit of ionic strength: Journal of Chemical Education, v. 78, n. 12, p. 1691–1692, http://dx.doi.org/10.1021/ed078p1691
Song, X. P., Wang, S. W., Chen, L., Zhang, M. L., and Dong, Y. H., 2009, Effect of pH, ionic strength and temperature on the sorption of radionickel on Na-montmorillonite: Applied Radiation and Isotopes, v. 67, n. 6, p. 1007–1012, http://dx.doi.org/10.1016/j.apradiso.2009.02.085
Spencer, W. F., and Gieseking, J. E., 1954, Cobalt adsorption and release in cation-exchange systems: Soil Science, v. 78, p. 267–276, http://dx.doi.org/10.1097/00010694-195410000-00003
Sposito, G., 1984, Surface chemistry of soils: New York, Oxford University Press, 223 p.
——— 1992, The diffuse-ion swarm near smectite particles suspended in 1:1 electrolyte solutions: modified Gouy-Chapman theory and quasicrystal formation, *in* Güven, N., and Pollastro, R. M., editors, Clay-water interface and its rheological implications: Clay Minerals Society, CMS Workshop Lectures, v. 4, p. 127–156.
——— 1998, On points of zero charge: Environmental Science & Technology, v. 32, n. 19, p. 2815–2819, http://dx.doi.org/10.1021/es9802347
——— 2004, The surface chemistry of natural particles: New York, Oxford University Press, 242 p.
Stadler, M., and Schindler, P. W., 1993, Modeling of H^+ and Cu^{2+} adsorption on calcium-montmorillonite: Clays and Clay Minerals, v. 41, n. 3, p. 288–296, http://dx.doi.org/10.1346/CCMN.1993.0410303
Stumm, W., Huang, C. P., and Jenkins, S. R., 1970, Specific chemical interactions affecting the stability of dispersed systems: Croatica Chemica Acta, v. 42, p. 223–244.
Stumm, W., Hohl, H., and Dalang, F., 1976, Interaction of metal-ions with hydrous oxide surfaces: Croatica Chemica Acta, v. 48, p. 491–504.
Sverjensky, D. A., 1993, Physical surface-complexation models for sorption at the mineral-water interface: Nature, v. 364, p. 776–780, http://dx.doi.org/10.1038/364776a0
——— 2003, Standard states for the activities of mineral surface sites and species: Geochimica et Cosmochimica Acta, v. 67, n. 1, p. 17–28, http://dx.doi.org/10.1016/S0016-7037(02)01074-8
Tan, X. L., Hu, J., Zhou, X., Yu, S. M., and Wang, X. K., 2008, Characterization of Lin'an montmorillonite and its application in the removal of Ni^{2+} from aqueous solutions: Radiochimica Acta, v. 96, p. 487–495, http://dx.doi.org/10.1524/ract.2008.1515
Tazi, S., Rotenberg, B., Salanne, M., Sprik, M., and Sulpizi, M., 2012, Absolute acidity of clay edge sites from *ab-initio* simulations: Geochimica et Cosmochimica Acta, v. 94, p. 1–11, http://dx.doi.org/10.1016/j.gca.2012.07.010
Tertre, E., ms, 2005, Adsorption de Cs^+, Ni^{2+} et des lanthanides sur une kaolinite et une smectite jusqu'a 150°c: étude experimentale et modélisation, Laboratoire des Mécanismes et Transfert en Géologie: Toulouse, France, Université Paul Sabatier—Toulouse III, Ph. D. thesis, 259 p.
Tertre, E., Berger, G., Castet, S., Loubet, M., and Giffaut, E., 2005, Experimental sorption of Ni^{2+}, Cs^+ and Ln^{3+} onto a montmorillonite up to 150 °C: Geochimica et Cosmochimica Acta, v. 69, n. 21, p. 4937–4948, http://dx.doi.org/10.1016/j.gca.2005.04.024
Tertre, E., Beaucaire, C., Coreau, N., and Juery, A., 2009, Modelling Zn(II) sorption onto clayey sediments using a multi-site ion-exchange model: Applied Geochemistry, v. 24, n. 10, p. 1852–1861, http://dx.doi.org/10.1016/j.apgeochem.2009.06.006
Thoenen, T., 1999, Pitfalls in the use of solubility limits for radioactive waste disposal: The case of nickel in sulfidic groundwaters: Nuclear Technology, v. 126, p. 75–87.
Thomson, H. S., 1850, On the adsorbent power of soils: Journal of the Royal Agricultural Society of England, v. 11, p. 68–74.
Tiller, K. G., and Hodgson, J. F., 1960, The specific sorption of cobalt and zinc by layer silicates: Clays and Clay Minerals, v. 9, p. 393–403, http://dx.doi.org/10.1346/CCMN.1960.0090126
Tombacz, E., and Szekeres, M., 2004, Colloidal behavior of aqueous montmorillonite suspensions: the specific role of pH in the presence of indifferent electrolytes: Applied Clay Science, v. 27, n. 1–2, p. 75–94, http://dx.doi.org/10.1016/j.clay.2004.01.001
Tournassat, C., Neaman, A., Villiéras, F., Bosbach, D., and Charlet, L., 2003, Nanomorphology of montmorillonite particles: Estimation of the clay edge sorption site density by low-pressure gas adsorption and AFM observations: American Mineralogist, v. 88, n. 11–12, p. 1989–1995.
Tournassat, C., Ferrage, E., Poinsignon, C., and Charlet, L., 2004a, The titration of clay minerals. Part II.

Structural-based model and implications for clay reactivity: Journal of Colloid and Interface Science, v. 273, n. 1, p. 234–246, http://dx.doi.org/10.1016/j.jcis.2003.11.022

Tournassat, C., Greneche, J. M., Tisserand, D., and Charlet, L., 2004b, The titration of clay minerals. Part I. Discontinuous backtitration technique combined with CEC measurements: Journal of Colloid and Interface Science, v. 273, n. 1, p. 224–233, http://dx.doi.org/10.1016/j.jcis.2003.11.021

Tournassat, C., Chapron, Y., Leroy, P., Bizi, M., and Boulahya, F., 2009, Comparison of molecular dynamics simulations with Triple Layer and modified Gouy-Chapman models in a 0.1 M NaCl–montmorillonite system: Journal of Colloid and Interface Science, v. 339, n. 2, p. 533–541, http://dx.doi.org/10.1016/j.jcis.2009.06.051

Tournassat, C., Bizi, M., Braibant, G., and Crouzet, C., 2011, Influence of montmorillonite tactoid size on Na-Ca cation exchange reactions: Journal of Colloid and Interface Science, v. 15, n. 2, p. 443–454, http://dx.doi.org/10.1016/j.jcis.2011.07.039

Van Loon, L. R., and Glaus, M. A., 2008, Mechanical compaction of smectite clays increases ion exchange selectivity for cesium: Environmental Science & Technology, v. 42, n. 5, p. 1600–1604, http://dx.doi.org/10.1021/es702487m

Villiéras, F., Michot, L. J., Cases, J. M., Berend, I., Bardot, F., François, M., Gérard, G., and Yvon, J., 1997, Static and dynamic studies of the energetic surface heterogeneity of clay minerals, *in* Rudzinski, W., Steele, W. A., and Zgrablich, G., editors, Equilibria and Dynamics of Gas Adsorption on Heterogeneous Solid Surfaces: Studies in Surface Science and Catalysis, v. 104, ch. 11, p. 573–623, http://dx.doi.org/10.1016/S0167-2991(97)80074-2

Voice, T. C., Rice, C. P., and Weber, W. J., 1983, Effect of solids concentration on the sorptive partitioning of hydrophobic pollutants in aquatic systems: Environmental Science & Technology, v. 17, n. 9, p. 513–518, http://dx.doi.org/10.1021/es00115a004

Wanner, H., Albinson, Y., Karnland, O., Wieland, E., Wersin, P., and Charlet, L., 1994, The acid/base chemistry of montmorillonite: Radiochimica Acta, v. 66/67, p. 157–162.

White, G. N., and Zelazny, L. W., 1988, Analysis and implications of the edge structure of dioctahedral phyllosilicates: Clays and Clay Minerals, v. 36, n. 2, p. 141–146, http://dx.doi.org/10.1346/CCMN.1988.0360207

Wold, J., and Pickering, W. F., 1981, Influence of electrolytes on metal-ion sorption by clays: Chemical Geology, v. 33, n. 1–4, p. 91–99, http://dx.doi.org/10.1016/0009-2541(81)90087-5

Wolthers, M., Charlet, L., and Tournassat, C., 2006, Reactivity of bentonite. An additive model applied to uranyl sorption, *in* Lützenkirchen, J., editor, Surface Complexation Modelling: Interface Science and Technology, v. 11, ch. 20, p. 539–552, http://dx.doi.org/10.1016/S1573-4285(06)80064-5

Xu, D., Tan, X. L., Chen, C. L., and Wang, X. K., 2008a, Adsorption of Pb(II) from aqueous solution to MX-80 bentonite: Effect of pH, ionic strength, foreign ions and temperature: Applied Clay Science, v. 41, n. 1–2, p. 37–46, http://dx.doi.org/10.1016/j.clay.2007.09.004

Xu, D., Zhou, X., and Wang, X. K., 2008b, Adsorption and desorption of Ni^{2+} on Na-montmorillonite: Effect of pH, ionic strength, fulvic acid, humic acid and addition sequences: Applied Clay Science, v. 39, n. 3–4, p. 133–141, http://dx.doi.org/10.1016/j.clay.2007.05.006

Yang, S. T., Li, J. X., Lu, Y., Chen, Y. X., and Wang, X. K., 2009, Sorption of Ni(II) on GMZ bentonite: Effects of pH, ionic strength, foreign ions, humic acid and temperature: Applied Radiation and Isotopes, v. 67, n. 9, p. 1600–1608, http://dx.doi.org/10.1016/j.apradiso.2009.03.118

Yokoyama, S., Kuroda, M., and Sato, T., 2005, Atomic force microscopy study of montmorillonite dissolution under highly alkaline conditions: Clays and Clay Minerals, v. 53, n. 2, p. 147–154, http://dx.doi.org/10.1346/CCMN.2005.0530204

Zachara, J. M., and Smith, S. C., 1994, Edge complexation reactions of cadmium on specimen and soil-derived smectite: Soil Science Society of America Journal, v. 58, n. 3, p. 762–769, http://dx.doi.org/10.2136/sssaj1994.03615995005800030018x

Zachara, J. M., Smith, S. C., McKinley, J. P., and Resch, C. T., 1993, Cadmium sorption on specimen and soil smectites in sodium and calcium electrolytes: Soil Science Society of America Journal, v. 57, n. 6, p. 1491–1501, http://dx.doi.org/10.2136/sssaj1993.03615995005700060017x